

The Dynamic Impact of Land-Use Changes on Soil Organic Carbon

Liang Diao*

Jean-Sauveur Ay†

Valentin Bellassen‡

Abstract

This study investigates soil organic carbon (SOC) response to land-use changes (LUC) across Europe by integrating field data from the LUCAS survey with satellite-based Corine Land Cover (CLC) data. Employing a dynamic approach, we observe that SOC accumulation following conversions from cropland to grassland or forest is gradual (10–20 years) yet substantial, whereas SOC losses due to conversions to cropland are more immediate (63% occurs within the first 1.5 years). We provide country-specific emission factors that enhance the precision of national greenhouse gas inventories. Our analysis of SOC changes since 1990 reveals significantly greater carbon sequestration compared to current national greenhouse gas inventory. These findings illustrate the need for region-specific parameters to estimate SOC changes and provide a ready-made solution for EU member states to comply with the LULUCF regulation on this aspect.

Keywords: Land-Use Change; Soil Organic Carbon; Carbon Emission; Carbon Sequestration

*CESAER, INRAE, Institut Agro, Université de Bourgogne, France. E-mail: liang.diao@inrae.fr

†CESAER, INRAE, Institut Agro, Université de Bourgogne, France. E-mail: jean-sauveur.ay@inrae.fr

‡CESAER, INRAE, Institut Agro, Université de Bourgogne, France. E-mail: valentin.bellassen@inrae.fr

1 Introduction

The amount of organic carbon in soils globally is two to three times greater than the amount of carbon in the atmosphere (Trumbore 2009). It thus plays a pivotal role in regulating atmospheric carbon dioxide levels, improving soil structure, and reducing greenhouse gas emissions (Lal 2004, Smith et al. 2008). As a major factor affecting terrestrial carbon balance, land-use changes (LUCs) can profoundly impact the global carbon cycle (Eggleston et al. 2006). Recognizing this, the European Union (EU) has introduced a distinct target for land-based net carbon removals, aiming for 310 million tonnes of CO₂ equivalent by 2030, distributed as binding net removal national targets for the land use, land-use change and forestry sector (Hannes Böttcher et al. 2024).

In this context, understanding and evaluating the impact of LUCs on soil organic carbon (SOC) is essential for developing effective strategies that balance the demands of food security, biodiversity conservation, and greenhouse gas emissions. Countries need robust data to set realistic targets, track progress, and implement policies that contribute to global carbon reduction goals. One of the main challenges in estimating the impact of LUC on SOC emission or sequestration comes from the need to combine soil carbon data of high quality with thoughtful statistical models to recover relevant impacts (Somarathna et al. 2017; Chen et al. 2015; Stanley et al. 2023).

The empirical literature on the impact of LUCs on SOC can be divided into experimental and observational studies (Larsen et al. 2019). On the one hand, long-term field experiments allow researchers to consistently measure SOC variations and relate them to precisely controlled LUCs and land management. They are usually based on a limited set of plots and pedoclimatic conditions, so the associated results have high internal validity but low external validity (they are not readily transferable to other pedoclimatic conditions and land management practices). On the other hand, observational studies have higher external validity because the data are available for larger sets of pedoclimatic conditions, under actual land management and with a uniform methodology. The challenge for researchers is then to use consistent measures of SOC and to model unobserved variables that affect SOC and are correlated with LUC (e.g., climate, geology or local planning regulations). When omitted, such variables are known to confound the estimation of the causal impact of LUC on the plots that effectively experienced a LUC (Imbens and Rubin 2015).

The present study estimates the impact of LUC on SOC across the EU, by leveraging observational field data from the LUCAS survey. The control for confounding variables is operated from repeated soil measurements, under the assumption that these variables are mostly constant in time. This approach generally presents low precision because of the small number of LUCs observed between two SOC measurements (De Rosa et al. 2024). We mitigate this drawback by employing a machine learning model based on satellite data to predict LUCs that occurred before the first soil measurement, and estimate their effects on SOC variations computed from LUCAS. The resulting combined dataset, which spans the period from 1990 to 2018, provides a precise and robust foundation for evaluating SOC responses to LUCs over time, without carrying over the omitted variable

bias which comes with the classical substitution of space for time in cross-sectional studies.

We use this novel approach to produce upscaled estimates of SOC response over time for LUCAS points that effectively experience a LUC. Our results highlight the dynamic aspect of SOC variations, demonstrating that the effects of LUCs on SOC are neither uniform over time nor symmetric between LUCs. SOC dynamics following transitions from cropland to forest or grassland tends to be gradual, whereas SOC losses following conversion to cropland are much more immediate. In both cases, the change in SOC during the initial years is more significant and substantial, an effect that would otherwise be masked by smaller changes in later years in a non-dynamic setting, as in [De Rosa et al. \(2024\)](#).

Compared to the results in the current literature ([Poeplau et al., 2011](#)), our findings show that the times required to reach SOC equilibrium are shorter and the total SOC loss is smaller. Comparing our dynamic approach to the current “static” or “cross-sectional” approaches to estimating SOC changes shows that our dynamic approach generally yields smaller SOC loss for plots that experienced transitions to cropland and larger SOC accumulation for transitions from cropland to other land uses. The combination of field data with long time series of remote sensing data also captures greater variability across countries, allowing us to account for spatial heterogeneity and long-term SOC dynamics in reporting greenhouse gas (GHG) emissions or sequestration.

We then use our estimates to report country specific emission factors, compliant with the IPCC guidelines and the LULUCF Regulation, and ready for use in national GHG inventories. Our dynamic Tier 2 approach estimates significantly higher carbon sequestration (572 Mtc) compared to the Tier 1 or cross-sectional Tier 2 approaches currently used in national inventories (76 Mtc). The higher estimates are primarily driven by increased soil carbon accumulation resulting from transitions from cropland to grassland (an additional 290 MtC), cropland to forest (an additional 100 MtC), and forest to grassland (an additional 50 MtC) since 1990. These gains more than offset the greater soil losses associated with transitions from grassland to forest (an additional 150 MtC) and grassland to cropland (an additional 78 MtC). This higher estimate means that policies based on IPCC’s conservative estimates could be missing significant opportunities for carbon sequestration in land management. As a result, countries could adjust their land-use policies to enhance SOC storage through better and more targeted land-use choices, thereby making meaningful contributions to GHG mitigation.

This study makes several key contributions to the existing literature on SOC and LUCs. First, we utilize the extensive LUCAS-soil dataset, integrating it with CLC data to create a comprehensive temporal and spatial representation of SOC changes across the EU. Compared to prior studies that primarily focused on static or cross-sectional analyses ([Schneider et al. 2021](#)), our research employs a dynamic approach to account for LUC history and the temporal evolution of SOC.

Second, our study specifically focuses on marginal lands that have been voluntarily converted to another land-use, a sample that is often underrepresented in the literature despite being representative of actual LUCs ([Guo and Gifford 2002](#), [Don et al. 2011](#)). By examining these marginal

lands, we provide novel insights into SOC dynamics under different LUC trajectories, highlighting the potential impacts of LUC on SOC in regions and land plots that are more susceptible to be converted in the future. In addition, our estimators take into account changes in practices actually carried out by land managers to adapt to variations in carbon in relation to their bio-climatic and economic conditions.

Finally, our findings offer important policy implications by demonstrating the variable impacts of different LUCs on SOC. Several studies have underscored the need for tailored land management practices to maximize SOC retention and promote sustainability across the EU (Lal 2004, Tóth et al. 2007). Our study expands on these findings by providing a dynamic perspective, which better captures the temporal variations and long-term impacts of LUCs on SOC. The average SOC variation derived from the whole EU may mask the large differences between countries. This is why the EU has required country-specific estimates by 2027, which a majority of member states are still lacking. Our dynamic approach captures greater heterogeneity across countries, which emphasizes the need for region-specific policies that promote land-use practices enhancing SOC sequestration.

2 Materials and Methods

2.1 Soil Organic Carbon Variations

In assessing Soil Organic Carbon variations (Δ SOC) from repeated soil measurements, we leverage topsoil samples from the LUCAS-soil dataset, a 10% subset of the LUCAS survey collected in 2009 (2012 in Bulgaria and Romania), 2015, and 2018. The LUCAS program, an initiative to track changes in land-use and cover throughout the EU, incorporated a soil module in the EU Member States. As the most extensive, uniform collection of topsoil in the EU, the LUCAS project collected soil samples and supporting data by ground observation at around 22,000 points across a variety of land covers during each survey. All samples were analyzed for physical and chemical properties in a single laboratory using the same analytical methods to enhance data consistency.

Following De Rosa et al. (2024), we exclude sites with organic-rich soils ($\text{SOC} > 160 \text{ g C kg}^{-1}$), those with over 5% CaCO_3 , and those missing either SOC values or particle size analysis, leaving 16,680 points. LUCs are often inherently coupled with an alteration in bulk density. Therefore, we do not use the raw data on carbon content expressed in gC per kg of soil, but rather the total carbon stock in the first 20 cm expressed in tC per ha. This dependent variable is also more relevant as the carbon cost or benefit of a given LUC. Following De Rosa et al. (2024) and Pacini et al. (2023), total carbon stock is computed as follows:

$$\text{SOC}_t = \text{OC}_t \times \text{BDF} \times \text{DEPTH} \times (1 - \text{CVF}), \quad (1)$$

where SOC_t is the total carbon stock in the first 20 cm of soil at time t in tC.ha^{-1} ; OC_t is the

content of SOC in the fine soil in percentage in year t , BDF is the bulk density of the fine fraction of soil expressed in g.cm^{-3} as calculated in the following Equation 2; depth is 20cm; and CVF is the volume fraction occupied by coarse fragments in percentage from Equation 3 below.

$$\text{BDF} = \frac{MF}{VF} = \frac{\text{BDR} \times (1 - \text{CVF}) \times \rho C}{\rho C - \text{BDR} \times \text{CVF}} \quad (2)$$

$$\text{CVF} = \frac{VC}{VC + VF} = \frac{\text{CMF}}{\frac{\rho C}{\text{BDF}} + \left(1 - \frac{\rho C}{\text{BDF}}\right) \times \text{CMF}}. \quad (3)$$

The term BDR is the bulk density data obtained from Panagos et al. (2024) who developed an high-resolution map based on 6,000 LUCAS samples; CMF is the mass fraction occupied by coarse fragments in percentage sampled in LUCAS samples for each point at the time of the first data collection (2009 or 2015); VC is the volume of the coarse fragments in cm^3 ; VF is the volume of the fine fraction of soil in cm^3 ; MF is the mass of the fine fraction of soil in g; ρC is the density of the coarse fraction, which takes the value of 2.6 g.cm^{-3} .

2.2 Recovering Land-Use Changes

For LUCs, our methodology uses data from all five sequential waves of the LUCAS survey in 2006, 2009, 2012, 2015, and 2018, instead of only the three LUCAS-soil waves of 2009 (2012 in Bulgaria and Romania), 2015, and 2018. However, the LUCAS data have two shortcomings. First, it is short in duration, as it only permits analysis of the impacts of LUCs on SOC over 9 years at best,¹ while the literature suggests that it may take decades for soil carbon sequestration to reach equilibrium (Poeplau et al. 2011).² Second, while LUCAS includes around 1 million points all over the EU, it only selects about one-fourth of them in each wave due to its stratified sampling method (d’Andrimont et al. 2020). Therefore, most surveyed points do not have a full history of land use. To augment the temporal and spatial scope of our SOC response analysis, we adopt a machine learning model to predict ground-truthed LUCs - as observed in LUCAS - with CORINE Land Cover (CLC) data based on satellite observations and image treatments.

The CLC dataset at 100m resolution is distinguished from LUCAS by its reliance on satellite imagery interpretation rather than direct ground observations, thus exhibiting an overall accuracy level of 85% (Büttner et al., 2004; Feranec et al., 2007)). Nonetheless, this accuracy varies significantly across different land cover classifications. Particularly, agricultural areas characterized by dense vegetation and intricate cultivation patterns face challenges due to subjective photo interpretation (Haines-Young and Weber 2006). Hence, we train a machine learning (ML) model by aligning land cover data from CLC for the years 2006, 2012, and 2018 with concurrent data

¹ Assuming that the earliest possible LUC happens in 2007.5, the middle point of 2006 and 2009 and that the latest possible Δ SOC is observed in 2016.5, the middle point of 2015 and 2018.

² There is little empirical evidence to quantify how long it actually takes (see Falloon et al. 1998, Falloon et al. 2000, Tye et al. 2009 for limited long-run evidence).

from the LUCAS survey. This process is further enriched by incorporating ancillary information on soil types from the European Soil Database, slope and elevation data from the European Digital Elevation Model, and proximity to the nearest road and city from the Euro Global Map, along with local land cover heterogeneity.

The ML model is then utilized to estimate the probability of land-use being cropland, grassland, or forest for the years 1990 and 2000, a time-period not covered by LUCAS, and for the years 2006, 2012, and 2018, in cases where land-use information is missing from LUCAS. Specifically, we assign the land cover category with the highest probability to each point. If the highest probability among cropland, grassland, or forest does not exceed 50%, we label the points as “Other”. We achieve 70% accuracy for cropland, 65% for grassland, and 67% for forest. In Section A.3, we show the main results are robust to a bootstrap style sensitivity test (Rosenbaum, 2005).

2.3 Time Lag between LUC and Δ SOC

Armed with the ML predictions, we define LUC from X (eg. grassland) to Y (eg. cropland), hereafter LU_{XY} , a LUCAS-soil point which is set as X in all years prior to the LUC and as Y in all years after the LUC. There are a few missing values in 1990, 2009, and 2015, where neither CLC nor LUCAS data is available. This definition gives us 3,751 points with a single LUC, with 75% having occurred prior to the first LUCAS soil survey in 2009 (Figure A1) but only 6% having occurred prior to 2000.

We define an observation of the SOC change by $\Delta SOC_{t_1, t_2}$, where t_1 is the year of first observed SOC, t_2 is the year of the last observed SOC, and $\Delta SOC_{t_1, t_2}$ is the difference of the SOC between the two observations. As illustrated in Figure 1, we have at most two observations for each point: $\Delta SOC_{09,15}$ between 09 and 15, $\Delta SOC_{15,18}$ between 15 and 18. If SOC in 2015 is not available, we have only one observation and use $\Delta SOC_{09/12,18}$ between 09/12 and 18 instead.

Because some LUCAS-soil points can have multiple observations, 3,751 points yield 10,116 observations of $\Delta SOC_{t_1, t_2}$ for all LUCs, the majority being from cropland to grassland.

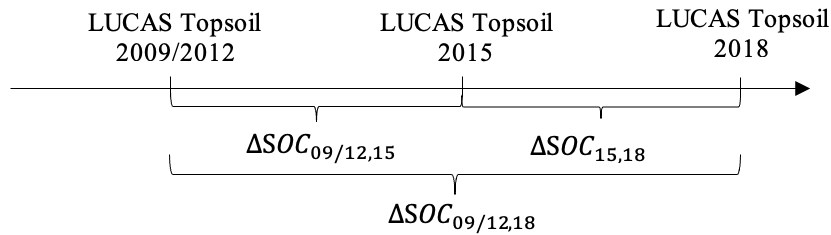


Figure 1: Illustration of the Three Different SOC Variations

We then exploit the timing of events to normalize the different numbers of years underlying $\Delta SOC_{t_1, t_2}$. If LUC occurred prior to the first measurement of SOC, the time length over which the

change in SOC is taking place is trivially the time difference between the two soil survey: $t_2 - t_1$. If LUC takes place in between two SOC measurements, the difference in SOC is thus entirely attributed to the LUC. The time length over which the change in SOC is taking place is therefore the time difference between LUC (t_{LUC}) and the second measurement of SOC: $t_2 - t_{LUC}$. The underlying assumption is that SOC was constant until LUC took place, that is between t_1 and t_{LUC} . Formally, we define $\Delta t = \min(t_2 - t_1, t_2 - t_{LUC})$. The annual average soil change is then calculated as: $\Delta SOC_{t_1, t_2} = (SOC_{t_2} - SOC_{t_1}) / \min(t_2 - t_1, t_2 - t_{LUC})$.

Since our observations often start several years after LUCs, we need to define the number of years passed since LUC for each observation. If LUC occurs prior to the first measurement as illustrated in Figure 2 (a), we assume the observed year of SOC change to be the midpoint of the interval between the two SOC measurements. The number of years passed since LUC is then defined as $(t_1 + t_2)/2 - t_{LUC}$. If LUC takes place in between two SOC measurements as illustrated in Figure 2 (b), we assume the observed year of SOC change to be the midpoint of the interval between the LUC and the second SOC measurement. The number of years passed since LUC is then defined as $(t_{LUC} + t_2)/2 - t_{LUC}$. Formally, we define Years Passed = $\max((t_1 + t_2)/2 - t_{LUC}, (t_{LUC} + t_2)/2 - t_{LUC})$. Table 1 shows the descriptive statistics of the processed data for all 6 types of LUCs.

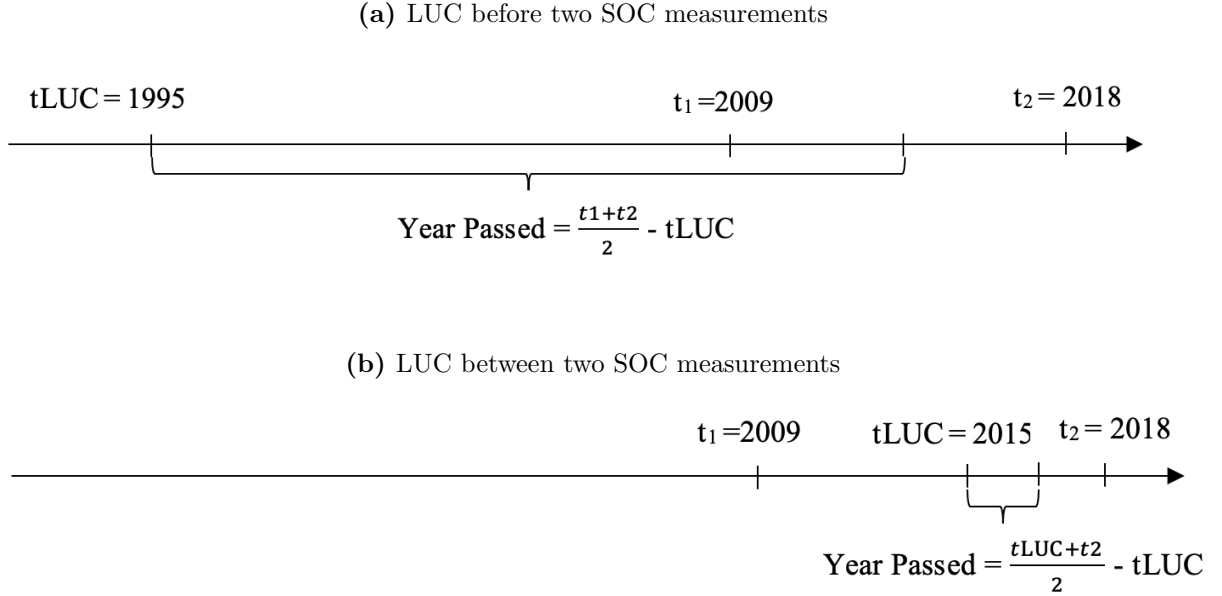


Figure 2: Illustration of the computation of Year Passed

2.4 Cumulative Δ SOC from LUCs

Previous computations allow us to relate yearly snapshots of Δ SOC to LUCs. To derive the cumulative change of SOC for a given LUC, we need to calculate the average Δ SOC for each time interval and to sum them for all the years before the equilibrium.

Table 1: Summary Statistics by Land-Use Change

LUC:	GC	FC	FG	CG	CF	GF
Initial SOC	41.5 (26.1)	32.7 (19.3)	47.8 (35.4)	51 (35.7)	65.6 (53.3)	56.8 (38.1)
Final SOC	39.9 (22.3)	32.8 (18.9)	49.8 (34.7)	53.4 (37.5)	71.1 (54.8)	61 (43.5)
Δ SOC per year	-.582 (5.89)	.108 (4.16)	.65 (7.95)	.778 (7.38)	1.37 (10.7)	1.25 (8.38)
N	704	450	775	1054	386	382

Standard errors in parentheses, * $p < 0.10$, ** $p < 0.05$, *** $p < 0.01$

Note: The table lists the mean and the standard deviation for 6 types of LUC, where G stands for Grassland; F stands for Forest, C stands for Cropland. Initial SOC is the carbon stock of the initial land-use in tC.ha^{-1} . Final SOC is the carbon stock of the final land-use in tC.ha^{-1} . Δ SOC per year is the annual average soil carbon change in $\text{tC.ha}^{-1}.\text{year}^{-1}$.

We thus define the time interval of each $\Delta\text{SOC}_{t_1, t_2}$ observation relative to the timing of LUC. Following Section 2.3, the relative timing of the first observation of SOC is $T_1 = \min(t_1, t_{LUC}) - t_{LUC}$ years since LUC and the second observation of SOC is $T_2 = t_2 - t_{LUC}$ years since LUC. Since different time intervals can overlap for different sites (Figure 3), we define the total average change of Δ SOC per year in time interval $[t_a, t_b]$ to be the weighted average of all $\Delta\text{SOC}_{i, T_1, T_2}$ per year that contain the time interval $[t_a, t_b]$:

$$\Delta\widehat{\text{SOC}}_{XY, t_a, t_b} = \frac{1}{n} \sum_{i=1}^n \Delta\text{SOC}_{i, T_1, T_2} \quad (4)$$

for all $\Delta\text{SOC}_{i, T_1, T_2}$ such that $T_1 \leq t_a, T_2 \geq t_b$ and $i \in LU_{XY}$

Take the example of Figure 3, there are three observations for land-use changes from grassland to cropland: ΔSOC_a , ΔSOC_b , and ΔSOC_c . For the time interval $[0, 1]$, $\Delta\widehat{\text{SOC}}_{GC, 0, 1} = \frac{1}{3}(\Delta\text{SOC}_{a, 0, 8} + \Delta\text{SOC}_{b, 0, 4} + \Delta\text{SOC}_{c, 0, 1}) * (1 - 0)$. Similarly, $\Delta\widehat{\text{SOC}}_{GC, 1, 4} = \frac{1}{2}(\Delta\text{SOC}_{a, 0, 8} + \Delta\text{SOC}_{b, 0, 4}) * (4 - 1)$ for the time interval $[1, 4]$. Using this definition, we derive the change of SOC based on $\Delta\widehat{\text{SOC}}_{XY, T_a, T_b}$ calculated in Equation (4) for each LUC XY and each time interval $[t_a, t_b]$ that are separated by year 0, 1.5, 3, 4.5, 6, 7.5, 9, 10.5, 12, 14, 15, 17, 20, 23.

2.5 Modeling spatial heterogeneity in LUC-related SOC changes

The dynamics of SOC response to LUCs can vary dramatically across climate zones and Eco-regions, given the large spatial extent of our analysis. To capture the heterogeneous response of SOC to LUCs across regions, we include the level of SOC, which can heavily influence the dynamics of Δ SOC following LUC (De Rosa et al. 2024). Thus, we estimate the following regression for each

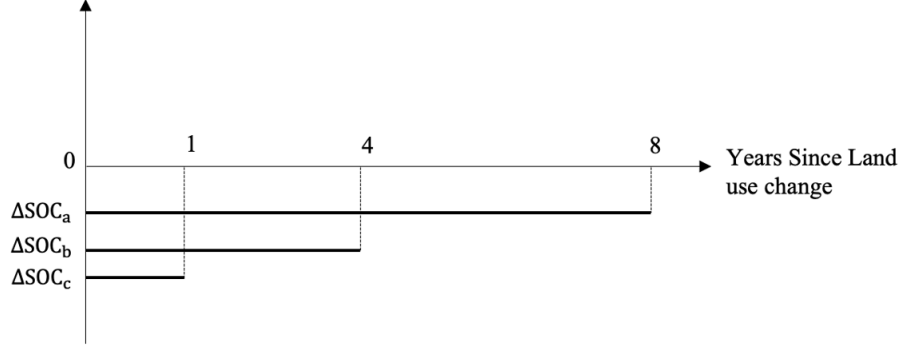


Figure 3: Illustration of Time Interval

218 LUC type:

$$\begin{aligned} \Delta SOC_{i,t1,t2} = & \alpha_t \text{Time Interval}_{i,t_a,t_b} + \beta_t \text{Time Interval}_{i,t_a,t_b} * \text{Final SOC}_{i,t2} \\ & + \gamma_t \text{Time Interval}_{i,t_a,t_b} * (\text{Final SOC}_{i,t2})^2 + \epsilon_i, \end{aligned} \quad (5)$$

219 where $\Delta SOC_{i,t1,t2}$ is the annual change in the soil organic carbon at point i between $t1$ and $t2$ as
 220 defined in section 2.3, $\text{Time Interval}_{i,t_a,t_b}$ is a dummy indicator taking value 1 if the time interval
 221 $[t_a; t_b]$ from the list of non-overlapping time intervals defined in section 2.4 is included in $[t_1; t_2]$
 222 and taking value 0 otherwise, and $\text{Final SOC}_{i,t2}$ is the carbon stock of the land-use at point i and
 223 time t_2 (always the final land use), assumed to be at equilibrium given the fast convergence of
 224 SOC following LUC in all six cases.³ To the extent that the final level of SOC heavily influences
 225 the dynamics of ΔSOC following LUC (De Rosa et al. 2024), we also include the interaction of
 226 $\text{Time Interval}_{i,t_a,t_b}$ and $\text{Final SOC}_{i,t2}$ as well as its squared term.

227 Some time intervals $[t_a; t_b]$ are only supported by a few points, making the coefficients of equa-
 228 tion (5) subject to over-fitting and low precision. To prevent this from happening, time intervals
 229 supported by fewer than 50 observations are merged with their neighbors prior to the estimation,
 230 until this all non-overlapping time intervals for each LUC XY are supported by at least 50 obser-
 231 vations. In addition, having several dummy variables equal to 1 for the same data point i (e.g.,
 232 ΔSOC_a in Figure 3) would bias the coefficients of equation (5) downwards. To avoid this, all
 233 points i concerned are replicated so that each replicate has a single dummy variable equal to 1.
 234 For example, ΔSOC_b in Figure 3 would be duplicated, with one replicate receiving value 1 for
 235 $\text{Time Interval}_{i,t_0,t_1}$ and the other receiving value 1 for $\text{Time Interval}_{i,t_1,t_4}$.

236 From the estimated OLS coefficients from (5), we then predict $\widehat{\Delta SOC}_{i,t_a,t_b}$ for each LUCAS
 237 point according to the different land uses. We assume the equilibrium year to be the first year
 238 when ΔSOC turns from positive to negative (or vice versa) for the first time.

³ Final SOC is used instead of initial SOC, because we do not observe the initial SOC if LUC took place before the first measurement at point i .

3 Results

3.1 Δ SOC Response to LUCs

We group the raw average Δ SOC estimates by the "years passed" and compute their standard deviations from sample variations. Figure A2 displays the results across all types of LUCs. Our large sample size allows us to detect small changes in SOC with high precision.

These raw averages are difficult to interpret because the time intervals covered by each point are not consistent, even for a given value of "years passed". The general picture is however consistent with our main results (with non-overlapping time intervals) presented in the next section. After transitions from grassland or forest to cropland, SOC decreases rapidly and reaches equilibrium within a relatively short time (i.e., less than few years, Figure A2a and A2c). In contrast, after cropland is converted to grassland or forest, and grassland to forest, SOC accumulates more gradually and over a longer period (about 10 years in Figure A2b, Figure A2d, and Figure A2f). Lastly, SOC changes following conversions from forest to grassland display no significant trend, with only minor insignificant fluctuations over time (Figure A2e).

From the computation described in Subsection 2.4, our main results are displayed in Figure 4 for all six types of LUC, where the shaded areas indicate the total amount of $\Delta \widehat{SOC}_{XY,t_a,t_b}$ in each time interval $[t_a, t_b]$, and the range indicates 95% confidence intervals.⁴ There seems to be rapid soil loss following the conversion from other land uses to cropland in the first 1.5 years – SOC decreases by 7 tC.ha⁻¹ following LUC from grassland to cropland, and 11.3 tC.ha⁻¹ following LUC from forest to cropland (Figure A1). The changes in SOC are negligible in the subsequent periods, with at most 37% of cumulated Δ SOC for the LUC (Figure 4a, 4c and Table 2).

On the other hand, we observe more gentle SOC accumulation following the conversion from cropland to other land uses. The initial soil accumulation in the first 1.5 years is smaller — SOC increases by 2.8 tC.ha⁻¹ following LUC from cropland to grassland, and 8.6 t C ha⁻¹ following LUC from cropland to forest, that is respectively 12 and 20% of cumulated Δ SOC (Table A1). But the impacts of LUC on SOC continue for longer duration, with sizeable soil accumulation until at least the 20th year (Figure 4b, 4d). Soil accumulation following LUC from grassland to forest presents a similar pattern. SOC increases by 8.38 tC.ha⁻¹ in the first 1.5 years, with sizeable soil accumulation until the 23rd year (Figure 4f). We observe no substantial change in SOC following a transition from forest to grassland as shown in Figure 4e.

These results improve the existing research based on observational data. Using the same LUCAS data, De Rosa et al. 2024 calculates the average changes of SOC in gC.kg⁻¹.year⁻¹ between 2009 and 2018 for GC and CG transitions. They find surprising results: the average change of SOC is much smaller right after LUC than 5–10 years later, and GC leads to positive Δ SOC. This

⁴The 95% confidence interval is calculated as $(\text{mean}(\Delta \widehat{SOC}_{i,T_a,T_b}) \pm 1.96 \times \text{standard deviation}(\Delta \widehat{SOC}_{i,T_a,T_b}))$ for each time interval $[t_a, t_b]$.

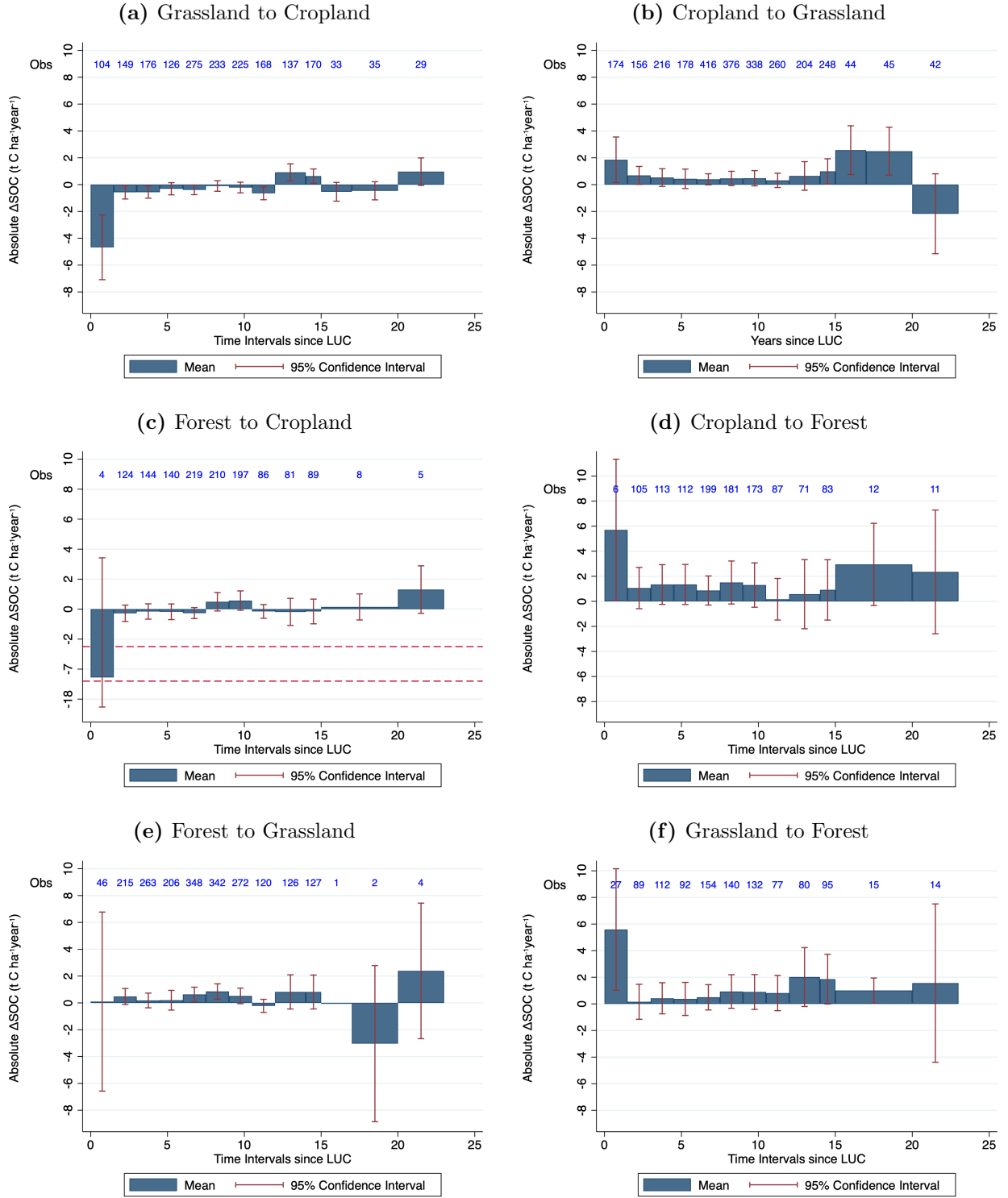


Figure 4: Δ SOC by time interval since LUC

Note: The Figure shows the soc variations predicted for each interval following a LUC. The values are computed from Equation 4.

is likely because frequent changes between temporary grassland and cropland, as well as land-use determination errors, blur the picture. Using CLC data, we focus on changes between permanent grassland and cropland, both reliably identified as such over the long term. This may explain why, despite using the same raw data on SOC, our results on Δ SOC and its first derivative have the expected signs (e.g. [Poeplau et al. 2011](#)). [Poeplau et al. \(2011\)](#) similarly find rapid soil loss in the initial years following other land uses to cropland, but only gradual soil accumulation following LUC of cropland to other land uses. To the contrary of [Poeplau et al. \(2011\)](#) however, our results show the soil loss reach the new equilibrium mostly within the first 1.5 years. [Poeplau et al. \(2011\)](#) mostly relies on paired sites instead of the more reliable chronosequences and its original studies have a lower time-resolution (3-6 years). For these reasons, and because we benefit from a larger sample size, we would argue that our figures are more accurate for the 0-20 cm horizon. However, the average depth of the studies reviewed by [Poeplau et al. \(2011\)](#) is larger than 20 cm, which could partly explain their slower time dynamics.

Table 2 displays the cumulated change in both absolute value and percentage relative to the initial SOC following all 6 types of LUCs (the cumulative sum stops at the first time-interval when the sign of Δ SOC changes or at 20 years, whichever occurs the soonest)⁵. Take the example of cropland to grassland in Figure 4b, the equilibrium is reached in the 20th year when Δ SOC becomes negative for the first time. Our estimates of % Δ SOC are similar to the results of [Poeplau et al. \(2011\)](#), except for transition from grassland to forest. In absolute values, our estimates are much larger the average Δ SOC reported in the national GHG inventories from 1990 to 2021.

Table 2: Δ SOC across LUCs

LUC	Δ SOC	Initial SOC	% Δ SOC	% Δ SOC Poeplau et al. 2011	Δ SOC GHG
CF	43.8 ± 19.9	66	66 ± 30	22.4 ± 10.4	16.8
CG	22.5 ± 7.4	53	42 ± 14	39.8 ± 11	9.6
GF	30.1 ± 11.3	59	51 ± 19	-4.0 ± 5.7	-0.1
FG	4.4 ± 17.9	46.9	9 ± 38		-2
FC	-12.6 ± 17.0	32.8	-38 ± 52	-31.4 ± 20.4	-21
GC	-11.1 ± 4.8	41.3	-27 ± 12	-36.1 ± 4.6	-10.9

Note: the table displays Δ SOC ($\text{tC.ha}^{-1} \pm 95\%$ Confidence Interval), the percentage change of Δ SOC ($\% \pm 95\%$ Confidence Interval), the percentage change of SOC reported in [Poeplau et al. 2011](#) over 20 years, and the change of SOC reported from the national GHG inventory following all six types of LUC ($\% \pm 95\%$ Confidence Interval, where G stands for Grassland; F stands for Forest, C stands for Cropland).

⁵ We use the bootstrapping method to obtain 95% confidence intervals. Taking the example of all points from cropland to grassland, we draw random samples with replacement from the dataset and calculate the absolute value of Δ SOC until a change in sign and within 20 years following the LUC. This process is repeated 1000 times, and the standard deviation is derived from the distribution of the 1000 absolute values of Δ SOC. The 95% confidence interval is then calculated as $(\text{mean} \pm 1.96 \times \text{standard deviation})$.

3.2 Country-level Δ SOC

The alteration of Figure A2 with a few merged intervals on which we estimate Equation 2.5 is presented in Figure A4. Table A2 to A7 in the Appendix show that the coefficients of Time Interval become smaller in magnitude and insignificant in later years, since the impact of LUC on Δ SOC decreases over time. Most coefficients of Time Interval interacted with the final SOC are significant and positive, indicating those land with higher levels of SOC have larger Δ SOC following LUC. This is consistent with previous findings from De Rosa et al. (2024) that plots with higher level of SOC tends to gain more from LUC.

In order to downscale the EU-scale values from Table 2, we use the estimated Equation (5) to predict the $\widehat{\Delta SOC}_{i,t_a,t_b}$ in each time interval $[t_a, t_b]$, using the average final SOC for each country and LUC type and the coefficients of Time Interval for each LUC type (listed in Table A2 to A7 in the Appendix). Summing up the predicted $\widehat{\Delta SOC}_{XY,t_a,t_b}$ in each time interval $[t_a, t_b]$ up until the first year when the sign changes, we derive the total change of Δ SOC for country and LUC type. These initial results seem rather unstable for all LUCs involving forests (Table A12). For some countries, either with a small number of plots for the given LUC or with an extremely low or high average SOC, the predicted values are too large to be realistic. Our interpretation is that three factors generate unstable predictions: 1) a small sample size for the LUC at EU level which may overfit the data for some time intervals; 2) a small sample size in the country, which may results in an average final SOC out of the calibration range of the model; and 3) inconsistencies in LUCAS-soil data with regards the inclusion of forest litter in the SOC values (Ran et al. 2010). Note that projected values at EU-level (see Figure A5) are sensible and similar to measured values (Figure A2), which is consistent with this interpretation.

Because of this instability, we forgo down-scaling for all LUCs involving forest, and recommend the use of values in Table 3 instead, where we country-level estimates with average Δ SOC values across the Europe Union derived from Figure A2 for all LUCs involving forest. Note that the CG estimates are surprisingly high in Latvia and the Netherlands. Grasslands in these countries have unusually high carbon stocks, possibly related to the abundance of wetlands and the difficulty to distinguish them from non-wet grasslands. Alternatively, the small sample sizes in these countries could also be an explanation. To the contrary, CG estimates are counter-intuitively negative in three mediterranean countries: Spain, Greece and Cyprus. The abundance of permanent croplands such as olive groves in these countries may explain this peculiarity. Conversion of irrigated cropland to rainfed grassland could also lead to SOC losses.

3.3 Comparing cross-sectional and dynamic approaches

It is worth noting that, to the contrary of the approach followed by most GHG inventories, our estimates of Δ SOC following LUC from X (e.g. cropland) to Y (e.g. grassland) are not the exact opposite of Δ SOC following the LUC from the opposite direction. This is true both for the

cumulated Δ SOC (Table 3) and the time-dynamics (Figure A2). The time-dynamics have been discussed in section 2.4. The differences in cumulated Δ SOC highlight that the plots that change in one direction are not comparable with those which change in the opposite direction. Based on our estimates, it seems that grasslands actually being converted to croplands have less carbon to loose on average than croplands actually being converted to grasslands (Table 3).

The “dynamic” estimates in Table 3, which leverage both the panel structure of the data and a reconstruction of LUC beyond the LUCAS survey, can then be compared with classical “static” or “cross-sectional” ones. To do so, we calculate the difference in SOC between each grassland point and its five nearest croplands, a protocol similar to Schneider et al. (2021) except that we do not control for soil chemical attributes and climate. Our replication results of Schneider’s protocol are displayed in Table A8. It yields similar estimates for Belgium and Estonia, the two countries for which the precise values are displayed in Schneider et al. (2021).⁶ Note that despite the static approach is not immune to surprisingly large estimates when performed on a per country and per LUC basis (e.g., -71 and -95 tC.ha⁻¹ for GC transitions in Croatia and Sweden respectively).

Table A9 shows the difference in Δ SOC estimated using our “dynamic” and “static” approaches. In general, our “dynamic” approach tends to yield higher increases and lower decreases in SOC than the “static” approach. There are larger SOC accumulation following LUCs from cropland or grassland to forest, and smaller SOC loss following LUCs from grassland or forest to cropland, and forest to grassland. The only counter-example is cropland to grassland where the “static” approach tends to predict higher accumulation. This discrepancy could again reflect the differences in considered plots. Indeed, the average SOC of plots that remain cropland throughout our sample is 36.7 tC.ha⁻¹, counter-intuitively much lower than the average initial SOC is 51 tC.ha⁻¹ and 65.6 tC.ha⁻¹ for plots that experience LUCs to grassland and forest respectively, as illustrated in Table 1. In this regard, the results obtained under this approach can better reflect the potential impacts of both past and potential LUCs on Δ SOC.

3.4 Comparison with officially reported values since 1990

To compare our results more directly with GHG inventories, panels (a) and (b) of Figure 5 consider the same LUCs from GHG inventories. The differences between the aggregated Δ SOC values are driven solely by the assumed impact of LUCs on Δ SOC (the total area which undergoes a given LUC is obtained from GHG inventories in both cases), and show strong disagreement between the two methods. From a release of -33 MtC in the GHG inventory, the UK shows a net sequestration of $+76.1$ MtC, mainly due to our higher value for sequestration from crop to grassland ($+80$ MtC in total) and a lower loss from grassland to crop ($+20$ MtC in total). For France, our estimates also reverse the net, with an estimated sequestration of $+80$ MtC from cropland to grassland, -25 MtC from grassland to cropland, while we find additional sequestration of $+50$

⁶ For Belgium SOC is 27.2 tC.ha⁻¹ (Schneider et al. 2021) vs 34.1 tC.ha⁻¹; For Estonia SOC is 5.2 tC.ha⁻¹ (Schneider et al. 2021) vs 18.6 tC.ha⁻¹)

Table 3: Δ SOC by Country and LUC under “Dynamic” Approach

Country/Region	Δ SOC _{GC}	N _{GC}	Δ SOC _{FC}	N _{FC}	Δ SOC _{FG}	N _{FG}	Δ SOC _{CG}	N _{CG}	Δ SOC _{CF}	N _{CF}	Δ SOC _{GF}	N _{GF}
AT	-8.7	1	-12.6	8	4.4	55	13.8	2	43.8	3	30.1	9
BE	-9.3	5	-12.6	2	4.4	3	33.6	4	43.8	1	30.1	3
BG	-9.5	10	-12.6	17	4.4	26	2.7	25	43.8	7	30.1	8
CY			-12.6		4.4	1	-22.2	1	43.8		30.1	
CZ	-15.8	3	-12.6	4	4.4	18	11.1	31	43.8	16	30.1	3
DE	-8.8	62	-12.6	20	4.4	31	24.1	82	43.8	47	30.1	20
DK	-11.0	2	-12.6	9	4.4	1	15.8	9	43.8	13	30.1	
EE	-11.5	1	-12.6	12	4.4	13	15.1	6	43.8	4	30.1	1
EL	-19.9	1	-12.6	9	4.4	27	-20.9	20	43.8	6	30.1	
ES	-8.4	21	-12.6	10	4.4	54	-23.4	38	43.8	8	30.1	45
FI			-12.6	29	4.4	12	18.7	5	43.8	13	30.1	
FR	-8.8	165	-12.6	12	4.4	42	25.3	83	43.8	17	30.1	37
HR	-8.6	1	-12.6		4.4	7	26.1	3	43.8		30.1	1
HU	-9.3	2	-12.6	4	4.4	3	26.1	16	43.8	7	30.1	1
IE	-8.3	3	-12.6		4.4	2	20.7	3	43.8		30.1	1
IT	-15.0	8	-12.6	12	4.4	42	5.7	31	43.8	3	30.1	2
LT	-9.5	19	-12.6	11	4.4	7	22.5	27	43.8	5	30.1	8
LU			-12.6		4.4		12.7	1	43.8		30.1	
LV	-8.5	5	-12.6	20	4.4	32	54.0	5	43.8	4	30.1	6
MT			-12.6		4.4				43.8		30.1	
NL	-8.6	6	-12.6		4.4		84.1	6	43.8	2	30.1	3
PL	-11.6	35	-12.6	20	4.4	18	1.4	116	43.8	43	30.1	28
PT	-17.9	12	-12.6	25	4.4	12	1.7	15	43.8	7	30.1	10
RO	-9.3	41	-12.6	10	4.4	41	2.3	72	43.8	4	30.1	37
SE	-17.3	1	-12.6	18	4.4	33	29.2	26	43.8	12	30.1	1
SI	-8.4	2	-12.6	3	4.4	14	25.7	3	43.8	2	30.1	2
SK	-9.6	2	-12.6	1	4.4	9	3.1	9	43.8	5	30.1	9
UK	-8.2	29	-12.6	2	4.4	9	32.1	33	43.8	2	30.1	17
Atlantic	-8.7	208	-4.6	16	50.4	56	29.8	130	59.3	22	22.3	61
Mediterranean	-12.5	43	-6.0	56	19.1	143	-9.7	108	-25.2	24	9.2	58
Scandinavian	-9.8	28	-6.4	99	11.7	98	25.2	78	27.6	51	-6.8	16
Continental	-9.7	158	-9.3	87	5.2	215	9.2	356	-1.8	134	19.5	117
European Union	-9.5	437	-7.2	258	15.3	512	12.0	672	8.1	231	16.1	252

Note: the table display Δ SOC (tC.ha⁻¹) and the number of observations under “dynamic” approach by Country following all 6 types of LUC, where G stands for Grassland; F stands for Forest, C stands for Cropland. For those countries that do not reach an equilibrium within 23 years following LUC, we show Δ SOC at the end of 23rd year. For LUCs involving forest, we use the average Δ SOC across EU calculated from Figure 4 due to small sample sizes and measurement inconsistency on forest floor. This is why the simulated EU value on the last line differs from the country-level values. See Table A12 for the original predicted country-specific values before replacement.

and +30 MtC for forest to grassland and crop to forest transitions, respectively. The reversal for Romania is almost exclusively due to our lower value for carbon emissions from a grassland to crop transition (-9.3 tC.ha^{-1}), whereas the GHG inventory considers a sequestration of $+7 \text{ tC.ha}^{-1}$ for this transition.

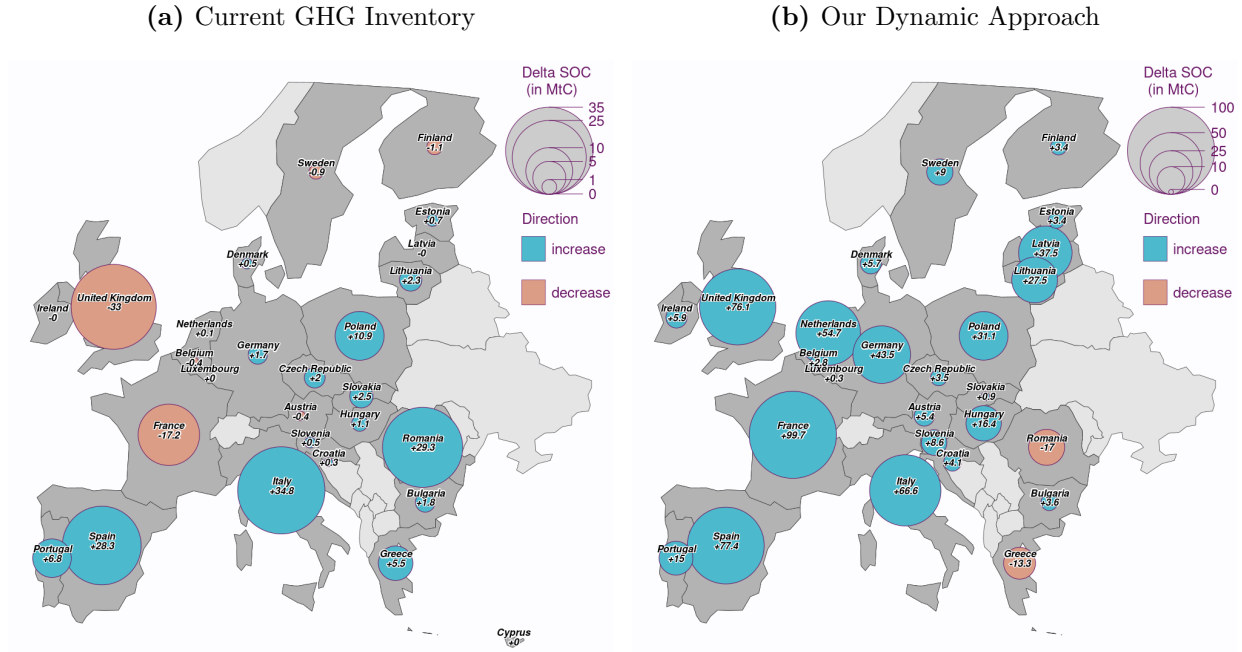


Figure 5: Δ SOC in MtC across some countries of EU, 1990-2018

Note: the Figure shows the total impacts of LUCs on SOC according to (a) current GHG inventory and (b) our dynamic approach. The two maps consider the same LUCs from GHG inventories.

At the EU scale, we estimate a much higher total SOC increase than GHG inventories (+ 494 MtC, see Table 4). The difference is mostly driven by the increased value of carbon sequestration from crop to forest (+100 MtC), crop to grassland (+101 MtC), and grassland to forest (+253 MtC) than in the GHG inventory. The latter comes from the common assumption in GHG inventories, in line with the IPCC Guidelines (Eggleston et al. 2006), that forests and grasslands have comparable SOC stocks. This is at odds with our observation based on LUCAS measurements that GF transitions generate an average cumulated increase of 30 tC/ha over the first 20 years. The other differences are driven by a combination of higher estimated cumulated Δ SOC (Table 2) and a difference in time dynamics: most GHG inventories assume linear changes which take 20 years to be completed whereas our estimates suggest that changes are concentrated over the first 1–5 years, and generally stop after 10–20 years.

Table 4: Total Δ SOC (MtC) since 1990 under “Dynamic” Approach and Current Inventory

Country	G to C	F to C	F to G	C to G	C to F	G to F	Total
“Dynamic” Approach	-139.6	-10.7	5.6	301.5	162.9	252.4	572.11
Current Inventory	-165.2	-18.1	-2.5	199.9	62.5	-0.5	76.1

Note: the table display total Δ SOC (MtC) under “dynamic” approach and current inventory, based on LUC changes since 1990 following all 6 types of LUC, where G stands for Grassland; F stands for Forest, C stands for Cropland.

3.5 Main limits

The most important limit in our approach is intrinsic to the use of LUCAS-soil measurements: despite all their advantages, they are limited to the 0–20 cm horizon. This should be sufficient to capture the big picture: 60–70% of total SOC is in the first 20 cm and more than 80% of SOC present at below 20 cm is not very reactive (average age higher than 10 years) (Balesdent et al., 2018). One could expect changes in SOC to be larger and slower for the entire soil profile, but the possibility of counter-intuitive redistributions as demonstrated for no/low till (Haddaway et al., 2017) cannot be ruled out.

Sample size is also a strong limit when investigating time-dynamics. We have 11 non-overlapping time intervals, six types of LUC and 28 countries, which generate risks of overfit and out-of-range predictions. To limit these risks, we merged intervals with too few data and use country-average SOC for predictions (less likely to be out-of-range than point-level SOC values). However, as we can see for LUCs involving forests, this may not yet be fully satisfactory. New LUCAS-soil waves will hopefully reduce this problem over time, although the proposed higher sampling intensity for LUCAS-soil would certainly help.

We can also expect that farming practices related to carbon management may differ from the results obtained from a model that does not really take practices into account, or that marginal plots that experience a LUC over the period are different in terms of geology, initial carbon stocks, or practices that other plots that do not experience a LUC.

4 Conclusion

This study underscores the significant impact of land-use changes (LUCs) on soil organic carbon (SOC) dynamics across European Union (EU). By integrating field data from the LUCAS survey with satellite data from Corine Land Cover (CLC), we developed a robust methodology to estimate SOC variations from observational data. Our method combines the best of the available EU data to ensure broad coverage of pedo-climatic conditions with actual land management. We also restrict our estimation to land plots that experienced a LUC over the period, which is shown to be important when the impacts are heterogeneous. Time-invariant confounding variables are accounted for by the

use of repeated soil measurements, which we enhance by coupling them with a Machine Learning (ML) model on a 28-year historical analysis of LUC.

The dynamic approach adopted in this study demonstrates that the impacts of LUC on SOC are larger than previously documented, especially for conversions to forest. Within the first 20 years, SOC increases by 37 tC.ha^{-1} following a transition from cropland to forest, and 26 tC.ha^{-1} following a transition from grassland to forest. In those cases of LUCs, the estimates are larger than previous findings in [Poeplau et al. \(2011\)](#). These insights are crucial for formulating effective land management policies aimed at enhancing carbon sequestration and mitigating climate change.

Furthermore, our findings reveal that the SOC response to LUC varies considerably across different types of land-use transitions and regions, highlighting the necessity for country-specific emission factors in compliance with IPCC guidelines. Although our proposal for such factors are still fragile for LUCs involving forests due to small sample sizes, they seem reliable for changes between cropland and grassland. In countries where a small sample size questions the genericity of the emission factor, the regional average can be used instead.

In conclusion, this study contributes to the growing body of literature on SOC dynamics following LUCs by providing a comprehensive, data-driven analysis of LUCs across the EU. The methodologies and findings presented here can aid policymakers in setting realistic targets for soil-based carbon sequestration, tracking progress, and implementing strategies that balance food security, biodiversity conservation, and GHG emissions. Future research should focus on refining these methods and expanding the dataset to include a larger sample of soil organic carbon measurements, especially for countries with small territories.

Author Contributions

Liang Diao: conceptualization, methodology, data curation, validation, formal analysis, supervision, visualization, project administration, writing – review and editing, writing – original draft. **Jean-Sauveur Ay:** conceptualization, methodology, supervision, funding acquisition, project administration, writing – review and editing, writing – original draft. **Valentin Bellassen:** conceptualization, methodology, data curation, validation, formal analysis, supervision, funding acquisition, visualization, project administration, writing – review and editing, writing – original draft.

Acknowledgment

This project benefited from funding by the European Union’s Horizon 2020 research and innovation program, EJP Soil projects Road4Scheme and SERENA (grant agreement No. 862695); ADEME, project “Impact des modes de production des produits alimentaires sous label sur la biodiversité” (BiodivLabel, grant agreement No. 2203D0043), the Bourgogne-Franche-Comté Region.

439 **Conflicts of Interest**

440 The authors declare no conflicts of interest.

References

- J. Balesdent, I. Basile-Doelsch, J. Chadoeuf, S. Cornu, D. Derrien, Z. Fekiacova, and C. Hatté. Atmosphere–soil carbon transfer as a function of soil depth. *Nature*, 559(7715):599–602, 2018.
- G. Büttner, J. Feranec, G. Jaffrain, L. Mari, G. Maucha, and T. Soukup. The CORINE land cover 2000 project. *EARSeL eProceedings*, 3(3):331–346, 2004.
- L. Chen, P. Smith, and Y. Yang. How has soil carbon stock changed over recent decades? *Global Change Biology*, 21(9):3197–3199, 2015.
- R. d’Andrimont, M. Yordanov, L. Martinez-Sanchez, B. Eiselt, A. Palmieri, P. Dominici, J. Gallego, H. I. Reuter, C. Joebges, and G. Lemoine. Harmonised LUCAS in-situ land cover and use database for field surveys from 2006 to 2018 in the European Union. *Scientific data*, 7(1):352, 2020.
- D. De Rosa, C. Ballabio, E. Lugato, M. Fasiolo, A. Jones, and P. Panagos. Soil organic carbon stocks in European croplands and grasslands: How much have we lost in the past decade? *Global Change Biology*, 30(1):e16992, 2024.
- A. Don, J. Schumacher, and A. Freibauer. Impact of tropical land-use change on soil organic carbon stocks—a meta-analysis. *Global Change Biology*, 17(4):1658–1670, 2011.
- H. S. Eggleston, L. Buendia, K. Miwa, T. Ngara, and K. Tanabe. 2006 IPCC guidelines for national greenhouse gas inventories. 2006.
- P. Falloon, P. Smith, K. Coleman, and S. Marshall. How important is inert organic matter for predictive soil carbon modelling using the Rothamsted carbon model? *Soil Biology and Biochemistry*, 32(3):433–436, 2000.
- P. D. Falloon, P. Smith, J. U. Smith, J. Szabo, K. Coleman, and S. Marshall. Regional estimates of carbon sequestration potential: Linking the Rothamsted Carbon Model to GIS databases. *Biology and Fertility of soils*, 27:236–241, 1998.
- J. Feranec, G. Hazeu, S. Christensen, and G. Jaffrain. Corine land cover change detection in Europe (case studies of the Netherlands and Slovakia). *Land use policy*, 24(1):234–247, 2007.

467 L. B. Guo and R. M. Gifford. Soil carbon stocks and land use change: A meta analysis. *Global*
468 *change biology*, 8(4):345–360, 2002.

469 N. R. Haddaway, K. Hedlund, L. E. Jackson, T. Kätterer, E. Lugato, I. K. Thomsen, H. B.
470 Jørgensen, and P.-E. Isberg. How does tillage intensity affect soil organic carbon? A systematic
471 review. *Environmental Evidence*, 6:1–48, 2017.

472 R. H. Haines-Young and J.-L. Weber. *Land Accounts for Europe 1990-2000: Towards Integrated*
473 *Land and Ecosystem Accounting*. Office for Office Publ. of the Europ. Communities, 2006. ISBN
474 92-9167-888-0.

475 Hannes Böttcher, Cristina Urrutia, Anke Herold, Sabine Gores, Etienne Mathias, Colas Robert,
476 Valentin Bellassen, Amelie Lindmayer, and Stephanie Wegscheider. Handbook on the updated
477 LULUCF Regulation EU 2018/841 - Guidance and orientation for the implementation of the
478 updated regulation - Version 2, 2024.

479 G. W. Imbens and D. B. Rubin. *Causal Inference in Statistics, Social, and Biomedical Sciences*.
480 Cambridge university press, 2015. ISBN 0-521-88588-4.

481 R. Lal. Soil carbon sequestration impacts on global climate change and food security. *science*, 304
482 (5677):1623–1627, 2004.

483 A. E. Larsen, K. Meng, and B. E. Kendall. Causal analysis in control–impact ecological studies
484 with observational data. *Methods in Ecology and Evolution*, 10(7):924–934, 2019.

485 R. Latifovic and I. Olthof. Accuracy assessment using sub-pixel fractional error matrices of global
486 land cover products derived from satellite data. *Remote sensing of Environment*, 90(2):153–165,
487 2004.

488 L. Pacini, F. Yunta, A. Jones, L. Montanarella, P. Barrè, S. Saia, S. Chen, and C. Schillaci. Fine
489 earth soil bulk density at 0.2 m depth from Land Use and Coverage Area Frame Survey (LUCAS)
490 soil 2018. *European Journal of Soil Science*, 74(4):e13391, 2023.

491 P. Panagos, D. De Rosa, L. Liakos, M. Labouyrie, P. Borrelli, and C. Ballabio. Soil bulk density
492 assessment in Europe. *Agriculture, Ecosystems & Environment*, 364:108907, 2024.

493 C. Poeplau, A. Don, L. Vesterdal, J. Leifeld, B. A. S. Van Wesemael, J. Schumacher, and A. Gensior.

- Temporal dynamics of soil organic carbon after land-use change in the temperate zone—carbon response functions as a model approach. *Global change biology*, 17(7):2415–2427, 2011.
- Y. Ran, X. Li, and L. Lu. Evaluation of four remote sensing based land cover products over China. *International Journal of Remote Sensing*, 31(2):391–401, 2010.
- P. R. Rosenbaum. Heterogeneity and causality: Unit heterogeneity and design sensitivity in observational studies. *The American Statistician*, 59(2):147–152, 2005.
- F. Schneider, C. Poeplau, and A. Don. Predicting ecosystem responses by data-driven reciprocal modelling. *Global Change Biology*, 27(21):5670–5679, 2021.
- P. Smith, D. Martino, Z. Cai, D. Gwary, H. Janzen, P. Kumar, B. McCarl, S. Ogle, F. O’Mara, and C. Rice. Greenhouse gas mitigation in agriculture. *Philosophical transactions of the royal Society B: Biological Sciences*, 363(1492):789–813, 2008.
- PDSN. Somarathna, B. Minasny, and B. P. Malone. More data or a better model? Figuring out what matters most for the spatial prediction of soil carbon. *Soil Science Society of America Journal*, 81(6):1413–1426, 2017.
- P. Stanley, J. Spertus, J. Chiartas, P. B. Stark, and T. Bowles. Valid inferences about soil carbon in heterogeneous landscapes. *Geoderma*, 430:116323, 2023.
- G. Tóth, V. Stolbovoy, and L. Montanarella. Soil quality and sustainability evaluation. *An integrated approach to support soil-related policies of the European Union. Office for Official Publications of the European Communities, EUR*, 22721, 2007.
- S. Trumbore. Radiocarbon and soil carbon dynamics. *Annual review of earth and planetary sciences*, 37:47–66, 2009.
- A. M. Tye, S. J. Kemp, and P. R. Poulton. Responses of soil clay mineralogy in the Rothamsted Classical Experiments in relation to management practice and changing land use. *Geoderma*, 153(1-2):136–146, 2009.

518 Appendix A: Appendix

519 A.1 Supplement Tables and Figures

Table A1: Cumulative Δ SOC by the Final Year of each Time Interval

Year	G to C	F to C	F to G	C to G	C to F	G to F
1.5	-7.0	-11.3	0.1	2.8	8.6	8.4
3	-7.9	-11.7	0.9	3.8	10.1	8.6
4.5	-8.7	-12.0	1.1	4.6	12.2	9.3
6	-9.2	-12.2	1.4	5.2	14.2	9.8
7.5	-9.8	-12.6	2.4	5.8	15.5	10.6
9	-9.9		3.7	6.5	17.7	11.9
10.5	-10.2		4.4	7.2	19.7	13.3
12	-11.2			7.7	19.9	14.5
14				9.0	21.1	18.5
15				10.0	22.0	20.4
17				15.1		
20				22.6	36.7	25.4
23					43.8	30.1

Note: the table show the cumulative Δ SOC (in tC ha⁻¹) by the final year of each time interval until SOC reaches the equilibrium or 6 LUC type.

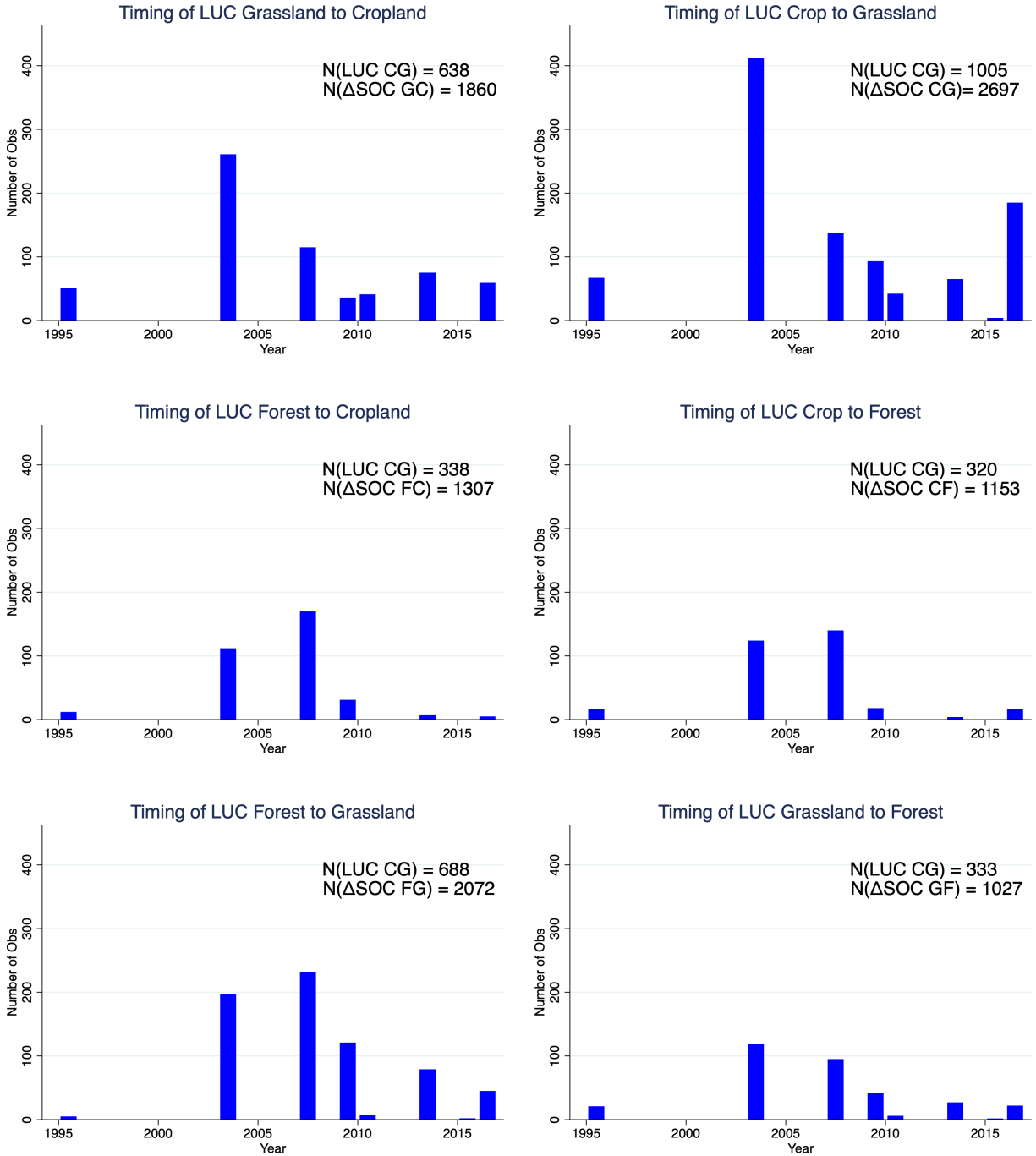


Figure A1: Distribution of LUC timings

Note: $N(\text{LUC } XY)$ is the number of LUCAS soil points experiencing a single change from X to Y over the sample period and $N(\Delta\text{SOC } XY)$ is the number of ΔSOC measurements for these points.

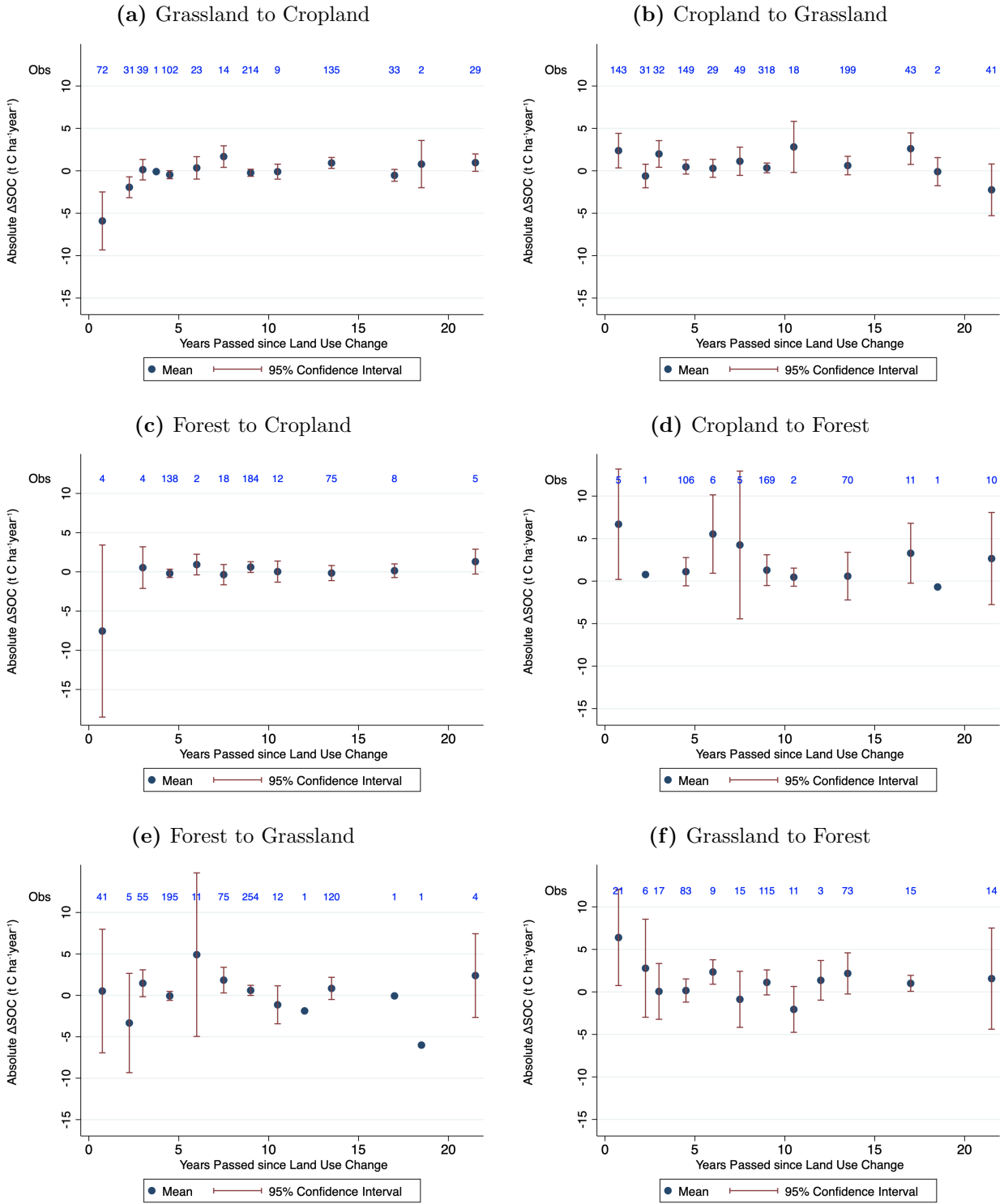


Figure A2: Δ SOC by number of years passed since LUC

Table A2: Impact of Cropland to Grassland change on Soil Organic Carbon

Dependent Variable:	Absolute change in SOC		
	(1) No X	(2) X SOC	(3) X SOC ²
Time Interval 0 - 1.5	-1.66 (1.01)	.0132 (.0335)	.00144*** (.000183)
Time Interval 1.5 - 3	-1.78 (1.11)	.0512* (.029)	-.0000655 (.00013)
Time Interval 3 - 4.5	-2.7*** (.94)	.0765*** (.0254)	-.000157 (.000119)
Time Interval 4.5 - 6	-2.63** (1.06)	.0705** (.0279)	-.000141 (.000126)
Time Interval 6 - 7.5	-1.75** (.74)	.0422** (.0191)	-.0000454 (.0000971)
Time Interval 7.5 - 9	-1.73** (.755)	.0392** (.0186)	4.15e-06 (.0000919)
Time Interval 9 - 10.5	-1.67** (.8)	.0362* (.0193)	.000018 (.0000937)
Time Interval 10.5 - 12	-1.98* (1.04)	.0466 (.0295)	-.0000802 (.000181)
Time Interval 12 - 14	-3.07*** (1.03)	.0377 (.026)	.00034*** (.00013)
Time Interval 14 - 17	-2.61*** (.889)	.035* (.0202)	.000264*** (.0000859)
Time Interval 17 - 23	-.871 (1.87)	-.0197 (.0359)	.000305** (.000126)
Observations	2697		

Standard errors in parentheses

* $p < 0.10$, ** $p < 0.05$, *** $p < 0.01$

Note: Dependent variable is the annual change in soil organic carbon. The table displays the results of a **single regression** in three columns: the coefficients of time intervals in column 1, the coefficients of time intervals interacted with final soil organic carbon in column 2, and the coefficients of time intervals interacted with squared final soil organic carbon in column 3.

Table A3: Impact of Grassland to Cropland change on Soil Organic Carbon

Dependent Variable:	Δ SOC		
	(1) No X	(2) X SOC	(3) X SOC ²
Time Interval 0 - 1.5	-2.96** (1.24)	-.069* (.0392)	.000486** (.000236)
Time Interval 1.5 - 3	-1.69 (1.04)	.0371 (.034)	-.000186 (.000213)
Time Interval 3 - 4.5	-1.68* (.936)	.0384 (.0317)	-.000197 (.000203)
Time Interval 4.5 - 6	-1.95 (1.4)	.0696 (.0631)	-.000536 (.000609)
Time Interval 6 - 7.5	-2.49*** (.855)	.096*** (.0337)	-.000824*** (.000277)
Time Interval 7.5 - 9	-2.56*** (.947)	.109*** (.0367)	-.00091*** (.000296)
Time Interval 9 - 10.5	-2.69*** (.979)	.108*** (.0377)	-.000891*** (.000301)
Time Interval 10.5 - 12	-2.83** (1.1)	.101** (.042)	-.000866*** (.00032)
Time Interval 12 - 14	-2.12 (1.33)	.0668 (.0559)	.000227 (.000504)
Time Interval 14 - 17	-1.23 (1.16)	.0178 (.0497)	.000537 (.000469)
Time Interval 17 - 23	.467 (3.77)	-.0539 (.195)	.00103 (.00225)
Observations	1860		

Standard errors in parentheses

* $p < 0.10$, ** $p < 0.05$, *** $p < 0.01$

Note: Dependent variable is the annual change in soil organic carbon. The table displays the results of a **single regression** in three columns: the coefficients of time intervals in column 1, the coefficients of time intervals interacted with final soil organic carbon in column 2, and the coefficients of time intervals interacted with squared final soil organic carbon in column 3.

Table A4: Impact of Cropland to Forest change on Soil Organic Carbon

Dependent Variable:	Absolute change in SOC		
	(1) No X	(2) X SOC	(3) X SOC ²
Year Passed 0 - 3	-3.47 (2.24)	.0446 (.0465)	.000142 (.000171)
Year Passed 3 - 4.5	-5.18** (2.21)	.0795* (.045)	.000031 (.000166)
Year Passed 4.5 - 6	-5.2** (2.21)	.0796* (.045)	.0000312 (.000166)
Year Passed 6 - 7.5	-2.3 (1.59)	.0153 (.0343)	.000248* (.000135)
Year Passed 7.5 - 9	.43 (1.67)	-.0369 (.0343)	.000441*** (.000128)
Year Passed 9 - 10.5	.458 (1.68)	-.0439 (.035)	.000475*** (.00013)
Year Passed 10.5 - 12	.501 (2.3)	-.0672 (.0575)	.000632** (.000268)
Year Passed 12 - 14	5.86** (2.98)	-.273*** (.0934)	.00216*** (.000582)
Year Passed 14 - 23	3.83 (2.4)	-.192*** (.0723)	.00168*** (.00043)
Observations	1153		

Standard errors in parentheses

* $p < 0.10$, ** $p < 0.05$, *** $p < 0.01$

Note: Dependent variable is the annual change in soil organic carbon. The table displays the results of a **single regression** in three columns: the coefficients of time intervals in column 1, the coefficients of time intervals interacted with final soil organic carbon in column 2, and the coefficients of time intervals interacted with squared final soil organic carbon in column 3.

Table A5: Impact of Forest to Cropland change on Soil Organic Carbon

Dependent Variable:	Absolute change in SOC		
	(1) No X	(2) X SOC	(3) X SOC ²
Year Passed 0 - 3	.794 (.899)	-.092** (.0425)	.00118*** (.000414)
Year Passed 3 - 4.5	-.112 (.891)	-.0428 (.0417)	.000934** (.00041)
Year Passed 4.5 - 6	-.0825 (.907)	-.0451 (.0423)	.000949** (.000414)
Year Passed 6 - 7.5	-.0498 (.73)	-.0421 (.0357)	.000863** (.000371)
Year Passed 7.5 - 9	1.09 (.664)	-.115*** (.0284)	.00211*** (.000238)
Year Passed 9 - 10.5	.835 (.678)	-.103*** (.029)	.00203*** (.000241)
Year Passed 10.5 - 12	-1.79 (1.64)	.0495 (.106)	.000199 (.00156)
Year Passed 12 - 14	-4.45*** (1.61)	.193* (.101)	-.00127 (.00142)
Year Passed 14 - 23	-4.57*** (1.5)	.212** (.0899)	-.00172 (.00121)
Observations	1307		

Standard errors in parentheses

* $p < 0.10$, ** $p < 0.05$, *** $p < 0.01$

Note: Dependent variable is the annual change in soil organic carbon. The table displays the results of a **single regression** in three columns: the coefficients of time intervals in column 1, the coefficients of time intervals interacted with final soil organic carbon in column 2, and the coefficients of time intervals interacted with squared final soil organic carbon in column 3.

Table A6: Impact of Forest to Grassland change on Soil Organic Carbon

Dependent Variable:	Absolute change in SOC		
	(1)	(2)	(3)
	No X	X SOC	X SOC ²
Year Passed 0 - 3	-4.67*** (.885)	.121*** (.0229)	-.000256** (.000104)
Year Passed 3 - 4.5	-1.72* (.894)	.0525** (.024)	-.00015 (.000105)
Year Passed 4.5 - 6	-2.27** (.985)	.0588** (.0276)	-.0000185 (.000112)
Year Passed 6 - 7.5	-1.89** (.797)	.0564*** (.0202)	-.0000705 (.0000867)
Year Passed 7.5 - 9	-2.45*** (.837)	.0862*** (.021)	-.000276*** (.0000892)
Year Passed 9 - 10.5	-2.4** (.94)	.0783*** (.0243)	-.000238** (.0000972)
Year Passed 10.5 - 12	-1.13 (1.46)	.0204 (.0371)	-.0000262 (.000157)
Year Passed 12 - 14	-2.98 (1.88)	.0546 (.0586)	.000242 (.000368)
Year Passed 14 - 23	-3.15* (1.84)	.0595 (.0571)	.000219 (.000361)
Observations	2072		

Standard errors in parentheses

* $p < 0.10$, ** $p < 0.05$, *** $p < 0.01$

Note: Dependent variable is the annual change in soil organic carbon. The table displays the results of a **single regression** in three columns: the coefficients of time intervals in column 1, the coefficients of time intervals interacted with final soil organic carbon in column 2, and the coefficients of time intervals interacted with squared final soil organic carbon in column 3.

Table A7: Impact of Grassland to Forest change on Soil Organic Carbon

Dependent Variable:	Absolute change in SOC		
	(1) No X	(2) X SOC	(3) X SOC ²
Year Passed 0 - 3	-4.09*** (1.58)	.0928** (.0401)	-.0000372 (.000192)
Year Passed 3 - 4.5	-4.85*** (1.55)	.106*** (.0399)	-.000191 (.000195)
Year Passed 4.5 - 6	-5.08*** (1.68)	.115*** (.0426)	-.000266 (.000207)
Year Passed 6 - 7.5	-2.22 (1.37)	.0196 (.0328)	.000208 (.000154)
Year Passed 7.5 - 9	-.667 (1.52)	-.0178 (.0372)	.000449** (.000188)
Year Passed 9 - 10.5	-1.06 (1.49)	-.0115 (.0371)	.000447** (.000188)
Year Passed 10.5 - 12	-.306 (1.84)	-.0364 (.045)	.000519** (.000214)
Year Passed 12 - 14	-.00582 (1.77)	-.0611 (.0406)	.000891*** (.000182)
Year Passed 14 - 23	-.522 (1.35)	-.0329 (.035)	.000794*** (.000167)
Observations	1027		

Standard errors in parentheses

* $p < 0.10$, ** $p < 0.05$, *** $p < 0.01$

Note: Dependent variable is the annual change in soil organic carbon. The table displays the results of a **single regression** in three columns: the coefficients of time intervals in column 1, the coefficients of time intervals interacted with final soil organic carbon in column 2, and the coefficients of time intervals interacted with squared final soil organic carbon in column 3.

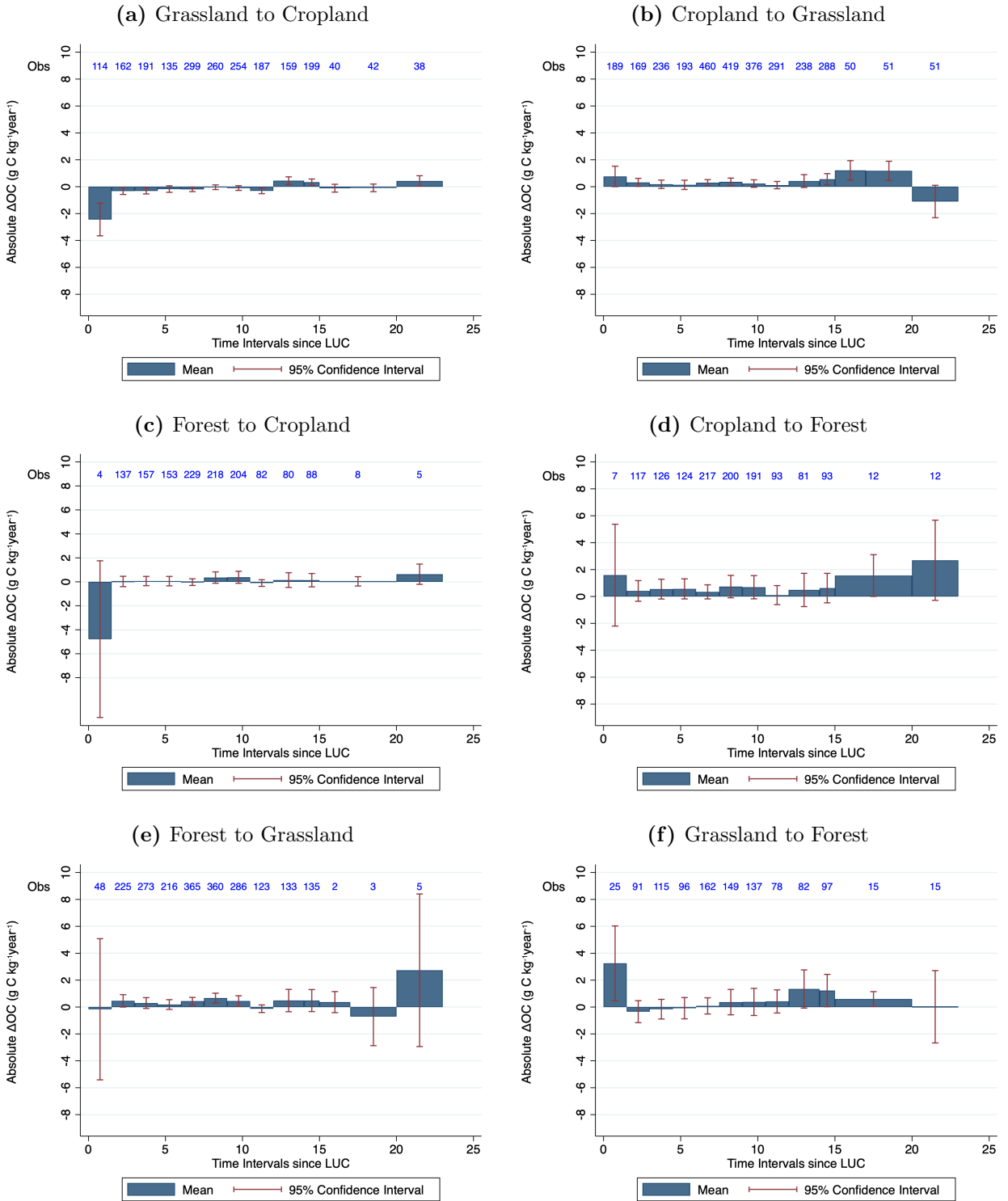


Figure A3: ΔOC by time interval since LUC

Note: The Figure shows the organic content variations (gC/kg soil, without bulk density) observed for each non-overlapping interval following a LUC. The values are computed from Equation 4.

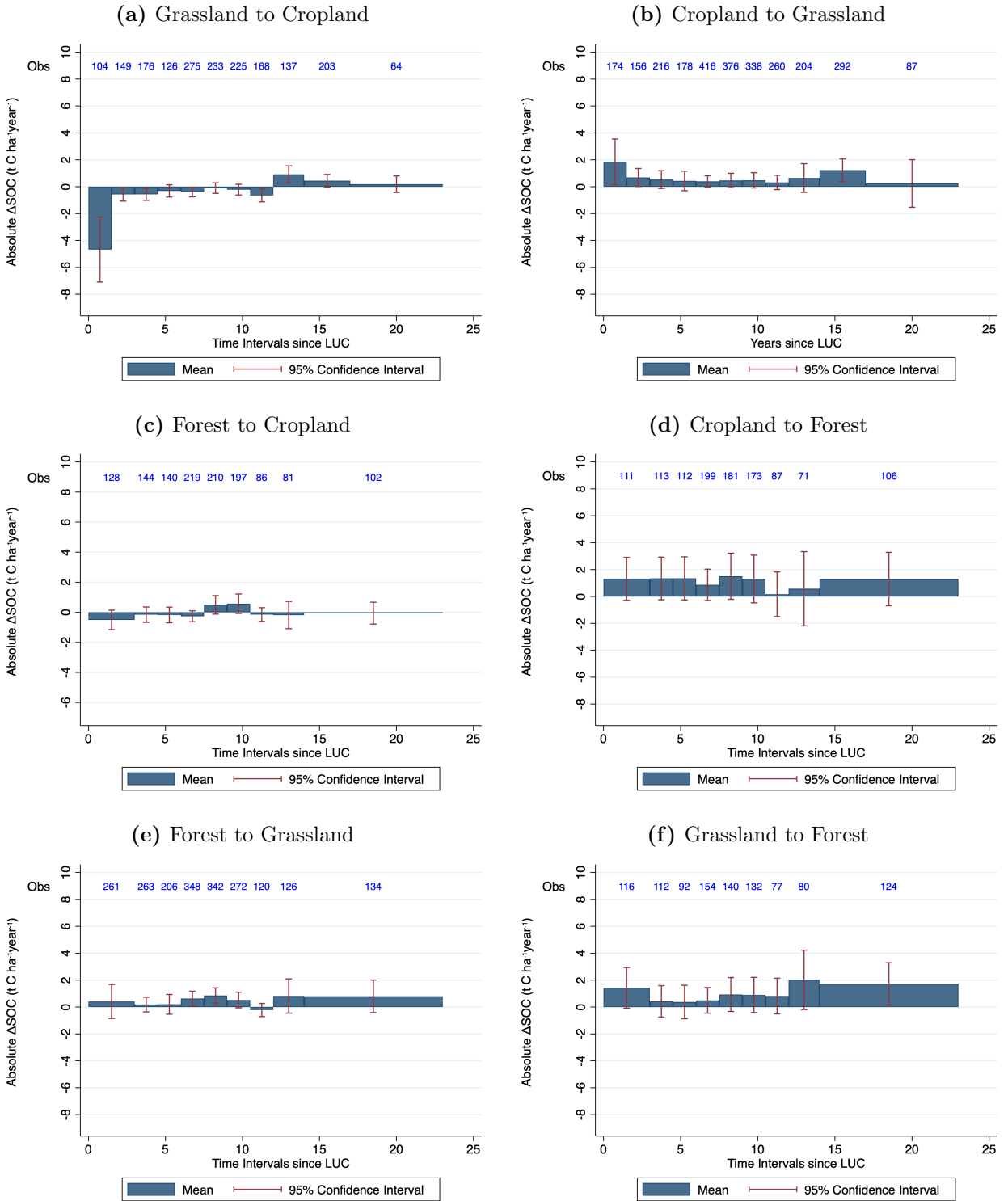


Figure A4: Δ SOC by time interval since LUC

Note: The Figure shows the soc variations predicted for each interval following a LUC. The values are computed from Equation 4.

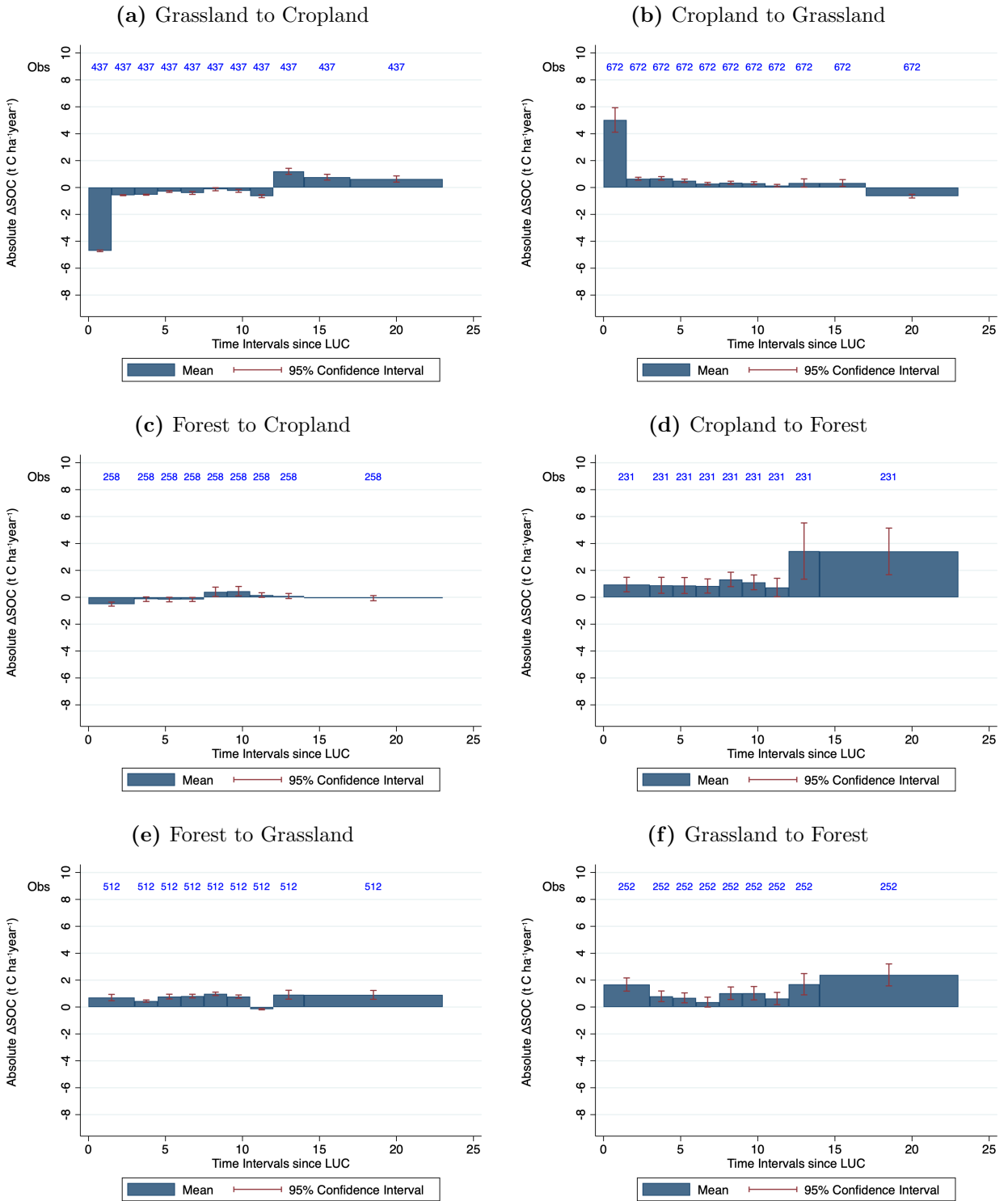


Figure A5: Δ SOC by time interval since LUC

Note: The Figure shows the Δ SOC predicted based on the regression analysis. The values are computed in Section 3.2.

Table A8: Δ SOC by Country and LUC under “Static” Approach

Country	G to C	F to C	F to G	C to G	C to F	G to F
AT	-38.9	-21.4	3.3	28.9	25.6	-4.4
BE	-45.3	-27.4	-4.7	33.3	31.9	-16.2
BG	-4.3	-11.9	-0.3	6.1	11.3	3.4
CY	-27.3	-28.7		-3.6	-33.2	
CZ	-15.5	-29.8	-18.6	2.1	26.4	10.4
DE	-50.9	-29.4	13.9	43.9	30.0	-14.0
DK	-53.5	-12.2		2.1	-43.3	
EE	-20.1	-29.5	29.5	33.5	19.6	-2.7
EL	-28.7	-29.3	6.4	37.6	32.8	3.4
ES	-26.4	-33.4	-6.5	26.7	35.0	4.3
FI	-10.8	3.2		-2.9	-14.2	
FR	-43.2	-31.3	-5.0	36.5	31.7	-6.0
HR	-71.2	-29.6	-1.2	46.4	25.4	-25.3
HU	-49.3	5.8	45.9	26.3	0.5	-59.9
IE	-52.5	-65.6	-14.7	54.4	86.2	30.8
IT	-29.0	-35.1	-7.1	22.7	25.0	-4.7
LT	2.3	-12.3	14.4	13.1	9.5	5.6
LU				7.0	-32.4	
LV	-4.2	-18.8	-12.2	-1.9	16.3	6.5
MT						
NL	-51.7	-3.8	33.0	33.0	-2.8	-11.2
PL	-47.5	-18.2	18.1	32.0	15.9	-24.7
PT	-12.9	-16.4	-2.7	20.2	21.0	4.0
RO	-3.2	-6.5	-2.3	5.0	7.9	-0.5
SE	-94.6	-14.4	94.4	90.4	-13.6	-85.0
SI	-29.1	0.0	45.0	48.6	3.5	-31.0
SK	-33.5	5.4	4.2	9.2	-2.0	-15.8
UK	-25.6	-6.7	3.1	30.6	31.2	-4.0

Note: the table display Δ SOC ($\text{tC}\cdot\text{ha}^{-1}$) under “static” approach by Country following all 6 types of LUC, where G stands for Grassland; F stands for Forest, C stands for Cropland.

Table A9: Difference of Δ SOC between “Dynamic” and “Static” Approach

Country	G to C	F to C	F to G	C to G	C to F	G to F
AT	30.2	8.8	1.1	-15.1	18.2	34.5
BE	36.0	14.8	9.1	0.3	11.9	46.3
BG	-5.2	-0.7	4.7	-3.4	32.5	26.7
CY		16.1			47.4	63.3
CZ	-0.3	17.2	23.0	9.1	17.4	19.7
DE	42.1	16.8	-9.5	-19.7	13.8	44.1
DK	42.5	-0.4			41.7	73.4
EE	8.5	16.9	-25.1	-18.5	24.2	32.8
EL	8.8	16.7	-2.0	-58.5	11.0	26.7
ES	18.1	20.8	10.9	-50.1	8.8	25.8
FI		-15.8			46.7	44.3
FR	34.4	18.7	9.4	-11.2	12.1	36.1
HR	62.6	17.0	5.6	-20.3	18.4	55.4
HU	40.0	-18.4	-41.5	-0.2	43.3	90.0
IE	44.3	53.0	19.1	-33.7	-42.4	-0.7
IT	13.9	22.5	11.5	-17.0	18.8	34.8
LT	-11.8	-0.3	-10.0	9.4	34.3	24.5
LU					36.8	62.5
LV	-4.3	6.2	16.6	56.0	27.5	23.6
MT						
NL	43.0	-8.8	-28.6	51.1	46.6	41.3
PL	35.9	5.6	-13.7	-30.6	27.9	54.8
PT	-5.0	3.8	7.1	-18.5	22.8	26.1
RO	-6.0	-6.1	6.7	-2.6	35.9	30.6
SE	77.3	1.8	-90.0	-61.2	57.4	115.1
SI	20.6	-12.6	-40.6	-22.9	40.3	61.1
SK	23.9	-18.0	0.2	-6.1	45.8	45.9
UK	17.4	-5.9	1.3	1.6	12.6	34.1

Note: the table show the difference of total Δ SOC (tC.ha^{-1}) under “dynamic” and “static” approach by Country following all 6 types of LUC, where G stands for Grassland; F stands for Forest, C stands for Cropland.

Table A10: Total Δ SOC (MtC) since 1990 under “Dynamic” Approach

Country	G to C	F to C	F to G	C to G	C to F	G to F
AT	-0.6	-0.1	0.2	1.1	1.1	3.7
BE	-1.5	-0.0	0.1	3.1	0.2	0.9
BG	-3.2	0.0	0.0	2.7	1.2	2.9
CY		-0.0	0.0	-0.0	0.0	0.0
CZ	-0.6	-0.0	0.0	2.8	0.8	0.5
DE	-14.1	-0.0	0.0	49.4	0.3	7.9
DK	-0.5	-0.1	0.0	1.6	4.5	0.2
EE	-0.3	-0.0	0.0	0.6	1.7	1.4
EL	-0.3	-0.0	0.0	-17.4	1.5	2.9
ES	-3.1	-2.9	0.2	-32.2	43.2	72.2
FI		-1.2	0.1	1.0	1.8	1.7
FR	-37.5	-4.6	3.2	57.3	42.7	38.6
HR	-0.5	-0.0	0.0	2.6	0.1	1.9
HU	-1.5	-0.1	0.0	3.6	12.7	1.7
IE	0.0	0.0	0.0	0.0	0.0	5.9
IT	-4.2	0.0	0.0	9.2	0.0	61.6
LT	-10.2	0.0	0.0	33.4	0.7	3.6
LU		-0.0	0.0	0.3	0.0	0.0
LV	-1.4	-0.1	0.2	32.5	2.5	3.8
MT		0.0	0.0		0.0	0.0
NL	-5.5	-0.1	0.2	58.1	0.7	1.3
PL	-0.5	0.0	0.0	0.4	27.3	3.9
PT	-2.5	-1.0	0.6	0.4	8.6	8.9
RO	-35.6	-0.3	0.2	11.9	2.8	4.0
SE	-0.8	-0.2	0.2	2.3	5.3	2.2
SI	-0.3	-0.0	0.1	2.3	0.0	6.5
SK	-0.3	-0.0	0.0	0.3	0.1	0.8
UK	-14.5	-0.0	0.2	74.2	3.0	13.2

Note: the table display total Δ SOC (MtC) under “dynamic” approach by Country, based on LUC changes since 1990 following all 6 types of LUC, where G stands for Grassland; F stands for Forest, C stands for Cropland.

A.2 Machine Learning Model

We train our machine learning model to predict whether each LUCAS point is cropland by CORINE data of the same year and location. To enhance the accuracy, we geo-reference the location by a set of input features listed in Table A11. Specifically, we include the four levels of administration division, the distance to the nearest settlement, city and road, soil type. Since the heterogeneity of local land cover can lower the accuracy of prediction (Latifovic and Olthof 2004), We aggregate the land cover surrounding each input point to determine the fraction representing the dominant land cover type, as well as the fraction that matches the land cover of the input point, following (Ran et al. 2010). We then split the dataset into five folds, train the cropland model by KNN algorithm with 50 nearest neighbours using four folds, and test the cropland model by the remaining fold. We repeat the same process and train the model for grassland and forest. Overall, our machine learning model achieves 85% accuracy in identifying the most likely 20% of cropland, 87% accuracy for the most likely 20% of forest, and 80% accuracy for the most likely 6.6% of grassland.

Table A11: Definitions and Sources for Input Features

Input Feature	Detail	Source
Latitude		LUCAS
Longitude		LUCAS
NUTS 0	country	LUCAS
NUTS 1	groups of states	LUCAS
NUTS 2	states	LUCAS
NUTS 3	groups of districts	LUCAS
Settlement Distance	the distance to the nearest settlement whose population is less than 50,000	EuroGlobalMap
City Distance	the distance to the nearest city whose population is larger than 50,000	EuroGlobalMap
Road Distance	the distance to the nearest road network	EuroGlobalMap
Soil type		ESDAC
	the land cover at the location of the input	
CORINE Land Cover	point in the raster file of 1990, 2000, 2006, 2012, and 2018	CORINE Land Cover
CORINE Reclassification	Reclassify CLC code 1-11 into Urban ; CLC code 12-17 into Crop; CLC code 18-21 and 26 into Grassland; CLC code 22-25 into Forest; CLC code 27-44 into Other	CORINE Land Cover
CORINE Neighbour	The number of neighbours (0-8) among eight directions (S, W, N, E, SW, SE, NW, NE) that have the same value as the central CORINE Land Cover	CORINE Land Cover
Dominant Land Cover	the fraction of dominant land cover within 1km of the input point	CORINE Land Cover
Same Land Cover	the fraction of the same land cover as the input point within 1km	CORINE Land Cover

EuroGlobalMap is accessed from <https://www.mapsforeurope.org/access-data>. ESDAC is accessed from <https://esdac.jrc.ec.europa.eu/content/european-soil-database-v20-vector-and-attribute-data>. CORINE Land Cover is accessed from <https://land.copernicus.eu/en/products/corine-land-cover>.

A.3 Robustness Tests

The results in Figure 4 are partially derived from our ML model, where we assign the land cover category with the highest probability to each point. To examine the quality of land-use predicted from the model as well as the CLC data it relies on, we conduct a bootstrap style test of sensitivity (Rosenbaum 2005). For 1990 and 2000 when land-use is not observed in LUCAS but predicted from CLC, land-use is randomly drawn based on the estimated probabilities instead of being attributed to the likeliest land-use possibility with a minimum likelihood of 50%. At each draw of the bootstrap, some ΔSOC values move in or out of the LUC_{XY} sample, proportionally to the probability that such a LUC actually occurred either between 1990 and 2000 or between 2000 and 2006. The process is repeated 100 times.

As illustrated in Figure A6, 100 simulations depicted by grey lines, derived from our machine learning model’s land-use predictions, exhibit a pattern consistent with the main result in Figure 4 represented by the red line. Note that each draw changes not only the estimates for the oldest LUCs, but also the most recent ones as a draw may drop some points which do not have 100% likelihood of having been the initial land-use both in 1990 and 2000. The positioning of the main result in the center of the distribution further validates our primary findings.

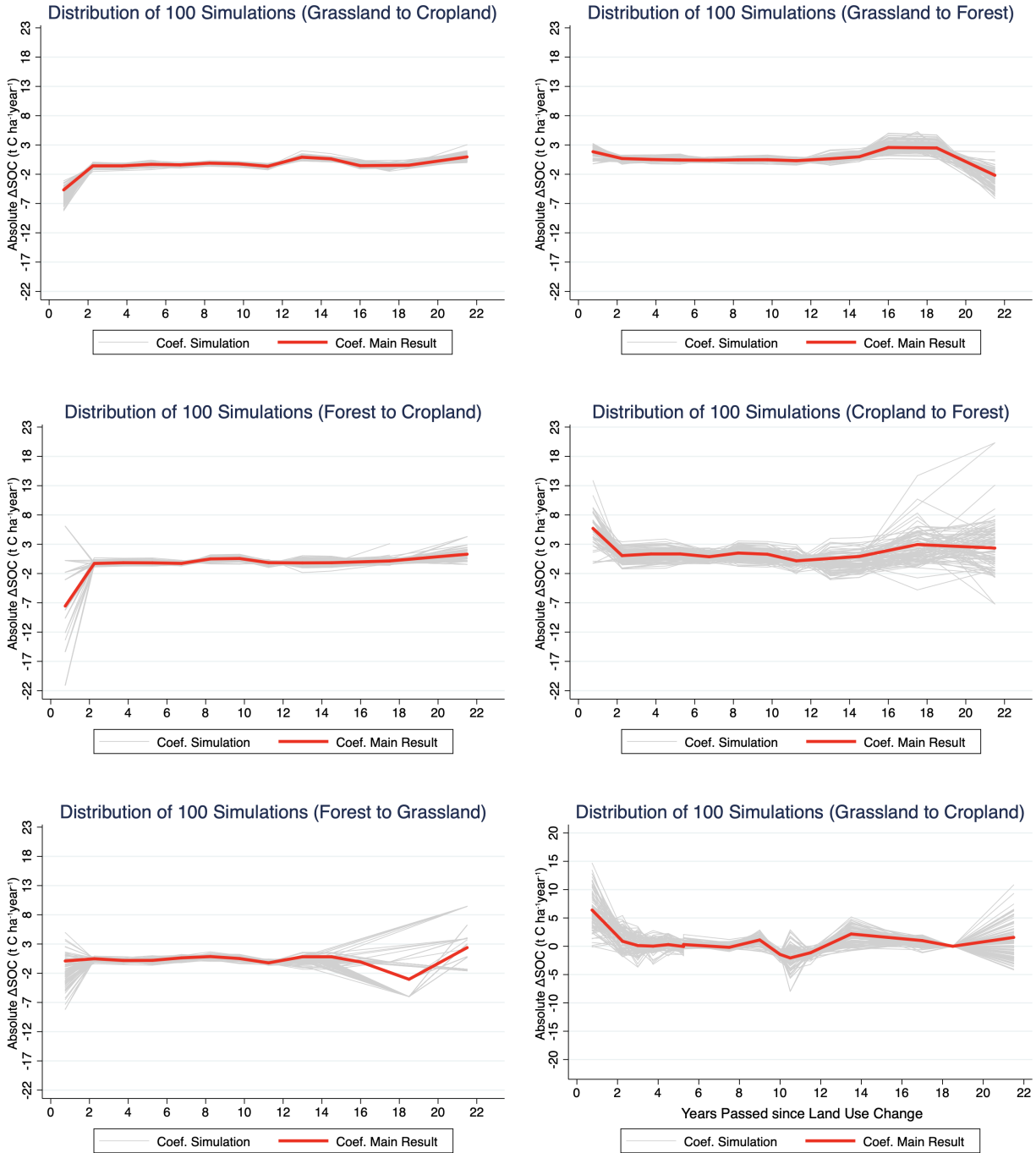
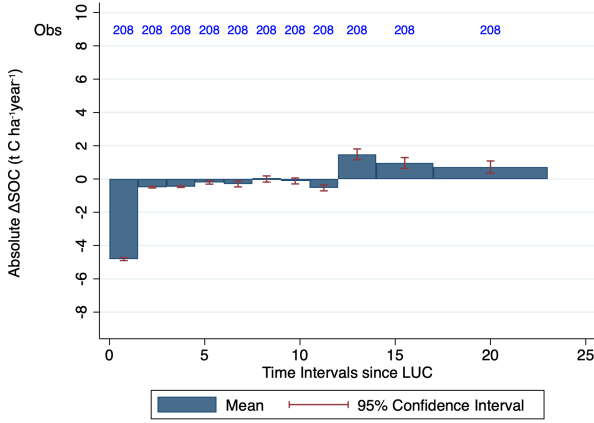


Figure A6: Simulation of Main Results

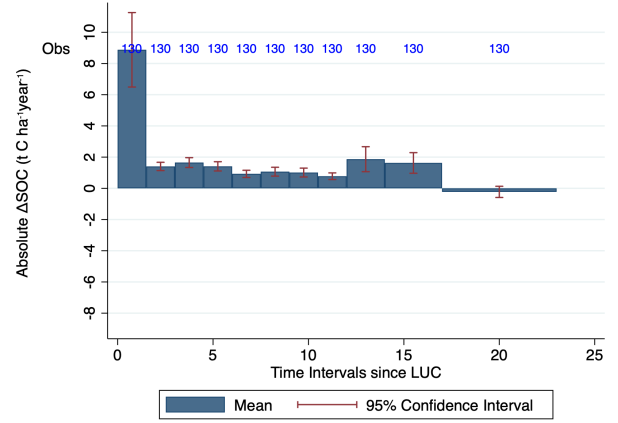
Table A12: Δ SOC by Country and LUC under “Dynamic” Approach

Country	Δ SOC _{GC}	N _{GC}	Δ SOC _{FC}	N _{FC}	Δ SOC _{FG}	N _{FG}	Δ SOC _{CG}	N _{CG}	Δ SOC _{CF}	N _{CF}	Δ SOC _{GF}	N _{GF}
AT	-8.7	1	-17.5	8	8.5	55	13.8	2	167.2	3	71.9	9
BE	-9.3	5	-2.2	2	4.4	3	33.6	4	288.0	1	17.5	3
BG	-9.5	10	-5.5	17	3.9	26	2.7	25	15.2	7	-12.4	8
CY			-28.2	1	-22.2	1						
CZ	-15.8	3	-7.0	4	-1.7	18	11.1	31	10.0	16	12.3	3
DE	-8.8	62	-6.6	20	11.5	31	24.1	82	15.3	47	78.2	20
DK	-11.0	2	-4.4	9	59.9	1	15.8	9	16.8	13		
EE	-11.5	1	-6.0	12	10.9	13	15.1	6	198.4	4	-34.3	1
EL	-19.9	1	-4.5	9	3.4	27	-20.9	20	-27.9	6		
ES	-8.4	21	-6.3	10	34.6	54	-23.4	38	-20.4	8	16.3	45
FI			-4.8	29	60.3	12	18.7	5	21.5	13		
FR	-8.8	165	-4.8	12	49.1	42	25.3	83	4.7	17	17.3	37
HR	-8.6	1			48.1	7	26.1	3			35.2	1
HU	-9.3	2	-12.5	4	-3.8	3	26.1	16	-29.0	7	705.4	1
IE	-8.3	3			-30.2	2	20.7	3			48.5	1
IT	-15.0	8	-6.2	12	11.6	42	5.7	31	-30.0	3	4.7	2
LT	-9.5	19	-13.7	11	-2.3	7	22.5	27	9.9	5	-15.2	8
LU							12.7	1				
LV	-8.5	5	-6.1	20	-0.3	32	54.0	5	1.2	4	6.8	6
MT												
NL	-8.6	6					84.1	6	57.7	2	5.8	3
PL	-11.6	35	-12.1	20	7.4	18	1.4	116	-29.9	43	-18.3	28
PT	-17.9	12	-6.4	25	-2.2	12	1.7	15	-26.3	7	-24.8	10
RO	-9.3	41	-6.4	10	-0.6	41	2.3	72	-30.0	4	0.7	37
SE	-17.3	1	-6.2	18	7.6	33	29.2	26	5.2	12	5.9	1
SI	-8.4	2	-16.4	3	8.9	14	25.7	3	14.2	2	8.7	2
SK	-9.6	2	-6.9	1	-0.8	9	3.1	9	-29.4	5	-11.6	9
UK	-8.2	29	-6.0	2	89.5	9	32.1	33	410.8	2	35.4	17
Atlantic	-8.7	208	-4.6	16	50.4	56	29.8	130	59.3	22	22.3	61
Mediterranean	-12.5	43	-6.0	56	19.1	143	-9.7	108	-25.2	24	9.2	58
Scandinavian	-9.8	28	-6.4	99	11.7	98	25.2	78	27.6	51	-6.8	16
Continental	-9.7	158	-9.3	87	5.2	215	9.2	356	-1.8	134	19.5	117
European Union	-9.5	437	-7.2	258	15.3	512	12.0	672	8.1	231	16.1	252

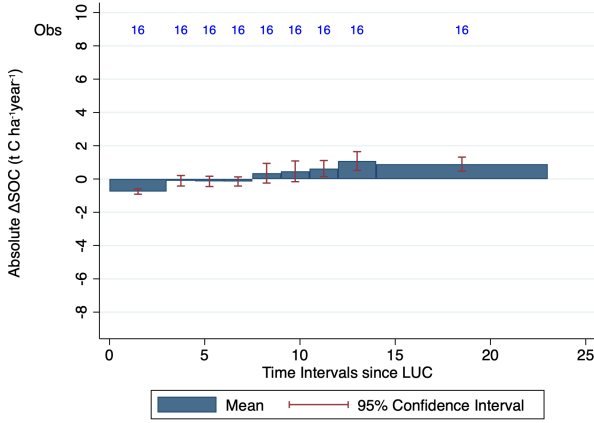
Note: the table display Δ SOC (tC.ha⁻¹) and the number of observations under “dynamic” approach by Country following all 6 types of LUC, where G stands for Grassland; F stands for Forest, C stands for Cropland. For those countries that do not reach an equilibrium within 23 years following LUC, we show Δ SOC at the end of 23rd year.



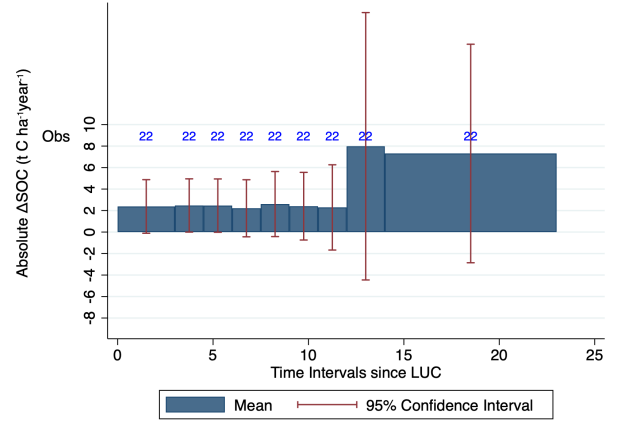
(a)



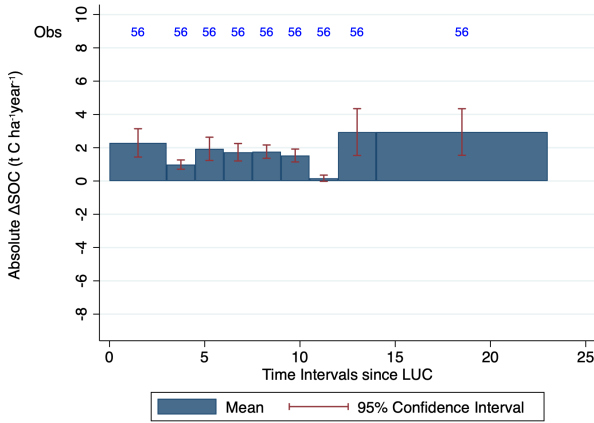
(b)



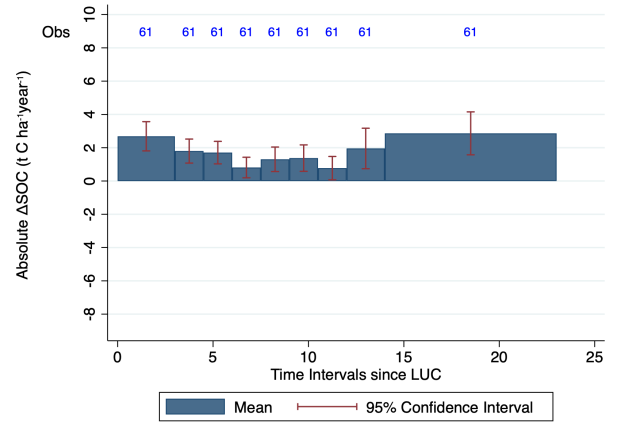
(c)



(d)



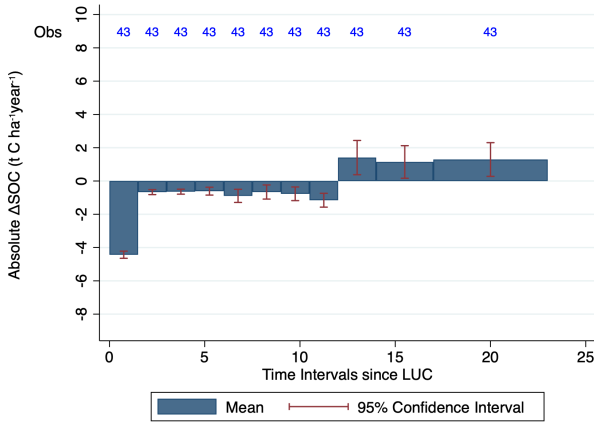
(e)



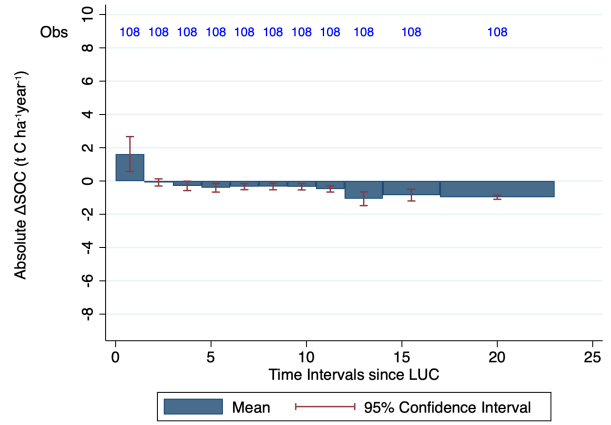
(f)

Figure A7: Δ SOC by time interval since LUC for Atlantic Region

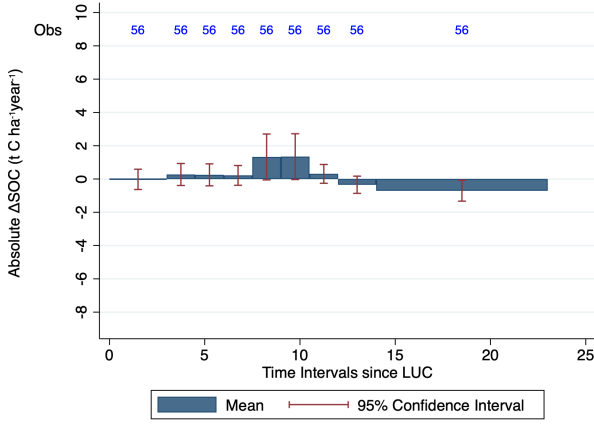
Note: The Figure shows the Δ SOC predicted based on the regression analysis. The values are computed in Section 3.2.



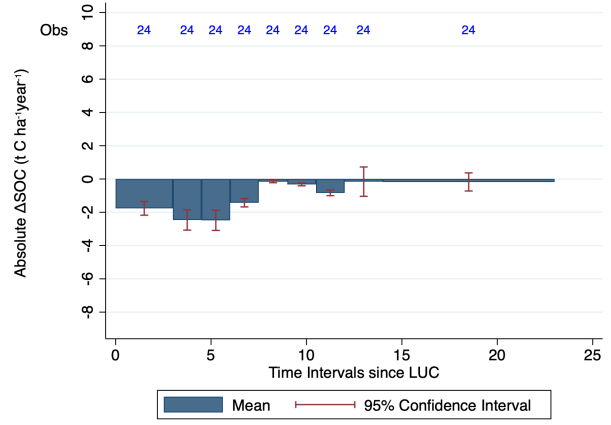
(a)



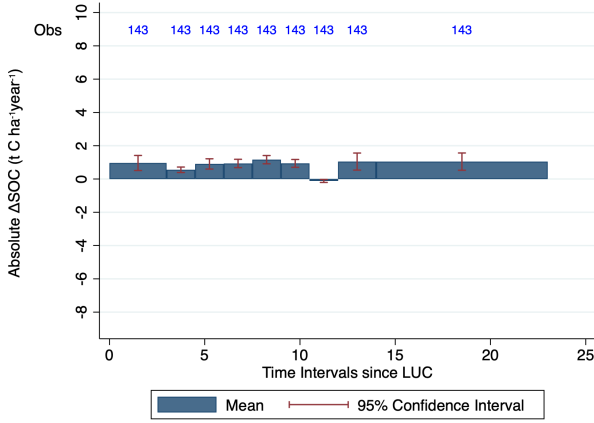
(b)



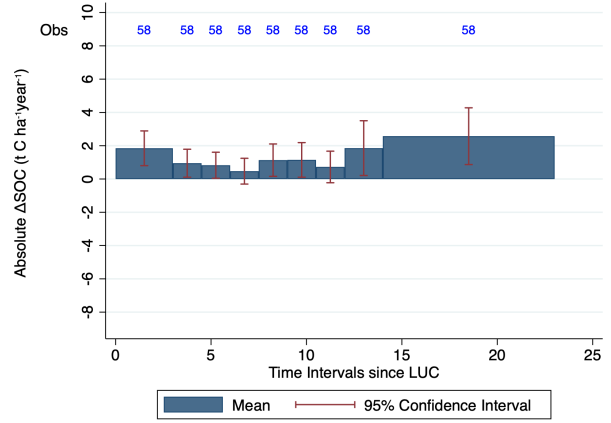
(c)



(d)



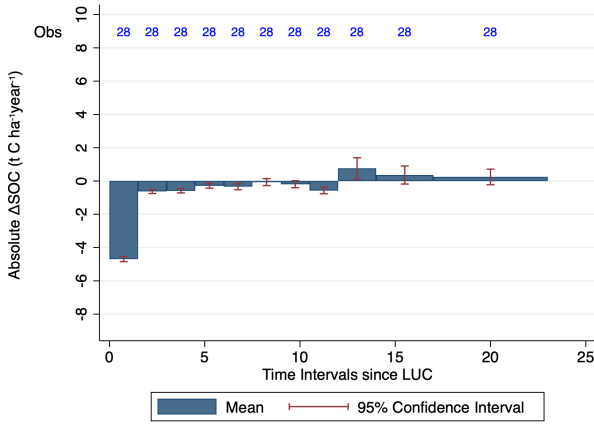
(e)



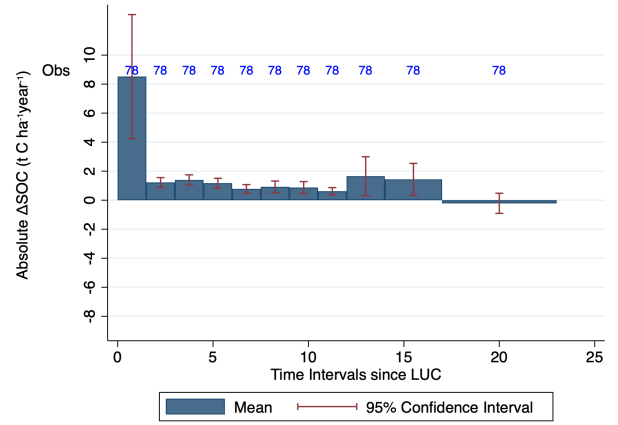
(f)

Figure A8: Δ SOC by time interval since LUC for Mediterranean Region

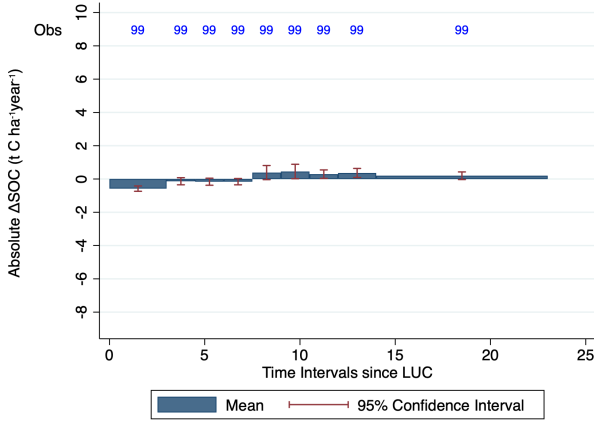
Note: The Figure shows the Δ SOC predicted based on the regression analysis. The values are computed in Section 3.2.



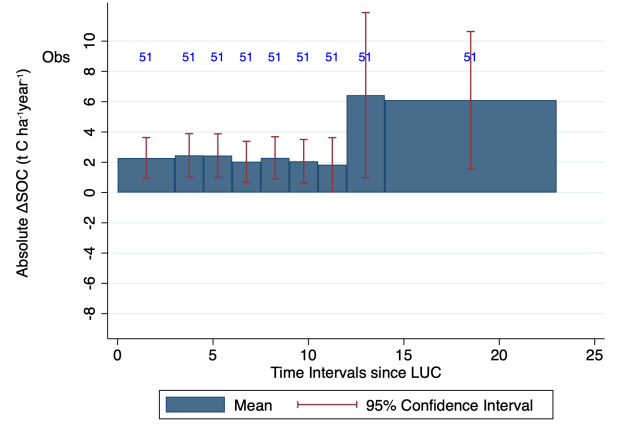
(a)



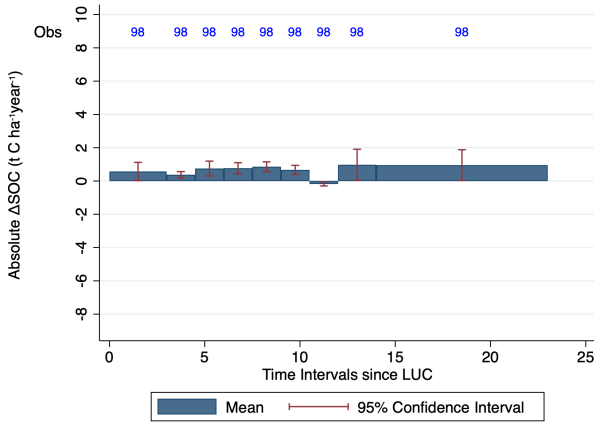
(b)



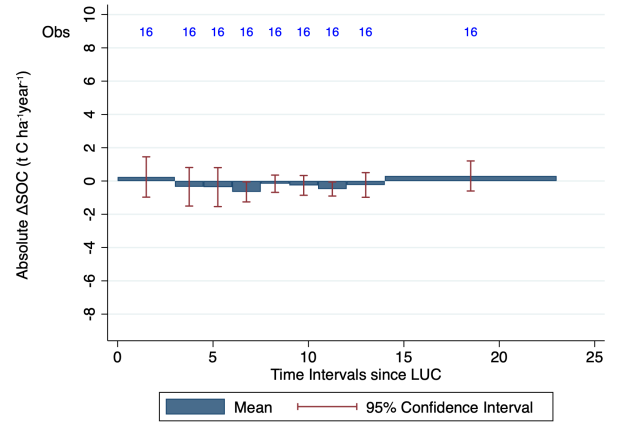
(c)



(d)



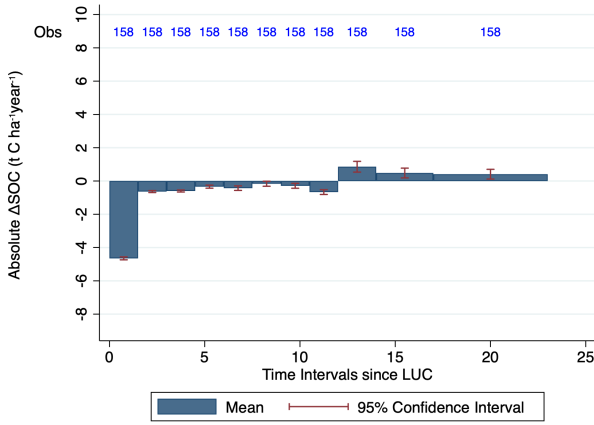
(e)



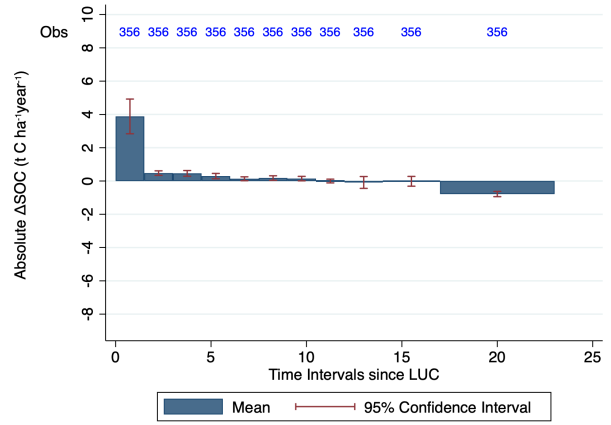
(f)

Figure A9: Δ SOC by time interval since LUC for Scandinavian Region

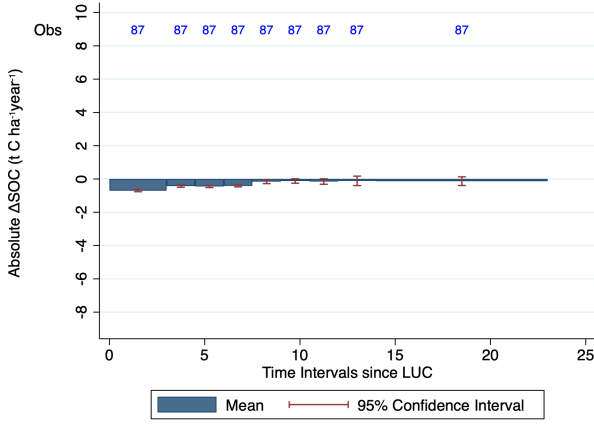
Note: The Figure shows the Δ SOC predicted based on the regression analysis. The values are computed in Section 3.2.



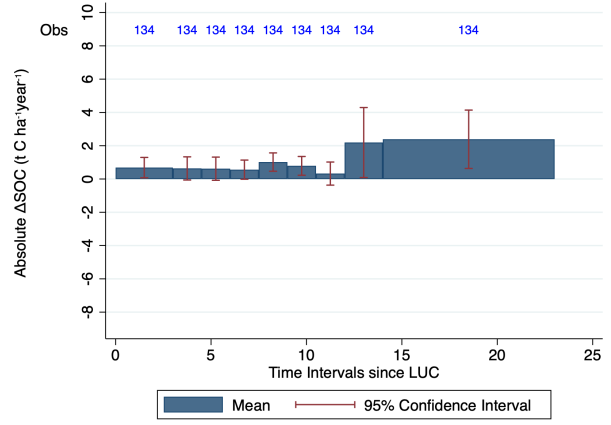
(a)



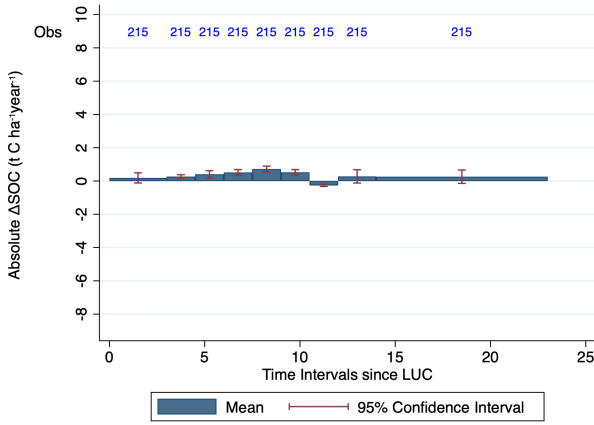
(b)



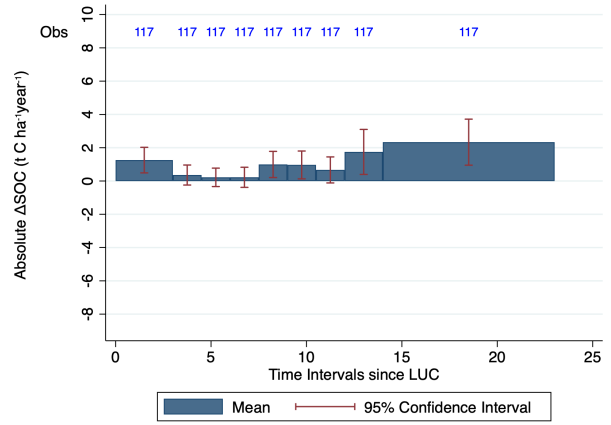
(c)



(d)



(e)



(f)

Figure A10: Δ SOC by time interval since LUC for Continental Region

Note: The Figure shows the Δ SOC predicted based on the regression analysis. The values are computed in Section 3.2.